DESIGN AND MODELLING OF $Ge_{11.5}As_{24}Se_{64.5}$ BASED MICROSTRUCTURED OPTICAL FIBER FOR SUPERCONTINUUM GENERATION

A PROJECT REPORT

Submitted in partial fulfillment of
the requirement for the award of the degree of

MASTER OF TECHNOLOGY
IN
MICROWAVE & OPTICAL COMMUNICATION

Submitted by:

Ankit Sharma
2K17/MOC/03

Under the supervision of

Dr. Ajeet Kumar
Assistant Professor

Department of Electronics and Communication
and
Department of Applied Physics

Delhi Technological University
(Formerly Delhi College of Engineering)
Bawana Road, Delhi-110042

JUNE 2019

DELHI TECHNOLOGICAL UNIVERSITY

(Formerly Delhi College of Engineering)

Bawana Road, Delhi – 110042

CANDIDATE'S DECLARATION

I, Ankit Sharma, Roll No. 2K17/MOC/03, student of M. Tech. in Microwave & Optical Communication, hereby declare that the project Dissertation titled "**Design and Modelling of $Ge_{11.5}As_{24}Se_{64.5}$ Based Microstructured Optical Fiber For Supercontinuum Generation**" which is submitted by me to the Department of Electronics and Communication and Department of Applied Physics, Delhi Technological University, Delhi in partial fulfillment of the requirement for the award of degree of Master of Technology, is original and not copied from any source without proper citation. This work has not previously formed the basis for the award of any Degree, Diploma Associateship, Fellowship or other similar title or recognition.

Place: Delhi

Date:

Ankit Sharma
2K17/MOC/03
M.Tech MOC

Department of Electronics and Communication
and
Department of Applied Physics
DELHI TECHNOLOGICAL UNIVERSITY
(Formerly Delhi College of Engineering)
Bawana Road, Delhi - 110042

CERTIFICATE

I hereby certify that the Project Dissertation titled "**Design And Modelling of $Ge_{11.5}As_{24}Se_{64.5}$ Based Microstructured Optical Fiber For Supercontinuum Generation**" which is submitted by Ankit Sharma, Roll No. 2K17/MOC/03, to the Department of Electronics and Communication and Department of Applied Physics, Delhi Technological University, Delhi in partial fulfillment of requirement for the award of the degree of Master of Technology in Microwave and Optical Communication Engineering, is a record of the project work carried out by the student under my supervision. To the best of my knowledge, this work has not been submitted in part or full for any Degree or Diploma to this University or elsewhere.

Dr. Ajeet Kumar
Assistant Professor
Department of Applied Physics
DTU

Prof. Rinku Sharma
(Head of Department)
Department of Applied Physics
DTU

Prof. S. Indu
(Head of Department)
Department of Electronics and Communication
DTU

ABSTRACT

Supercontinuum Generation (SCG) is a very exhilarating research field having multifarious applications in a variety of areas such as spectroscopy, medical imaging, telecommunication, high precision metrology and optical coherence tomography. The phenomenon of supercontinuum generation basically refers to the broadening of the spectrum of high intensity laser pulses as they traverse through a highly nonlinear medium. It was first reported in solid and gaseous nonlinear media by Alfano and Shapiro in the year 1970. The broadening of the spectra primarily takes place due to the interaction of linear effects such as dispersion as well as nonlinear phenomena involving self-phase modulation (SPM), cross-phase modulation (XPM), four-wave mixing (FWM), stimulated Raman scattering (SRS), and soliton dynamics at pump wavelength. SCG in the mid-infrared realm of wavelengths can play a pivotal role because mid-infrared spectroscopy has the capability to provide a thorough knowledge of the composition of molecular structures of the matter and executing non-intrusive diagnostics of diverse chemical, physical and biological systems.

In comparison to silica fibers, nonlinear materials like tellurite, bismuth, fluoride, and chalcogenides demonstrate significant optical nonlinearities and transparency in the near to mid-infrared realm of wavelengths which makes them quite apt for MIR supercontinuum generation. However, owing to optical transparency up to 25 μm in the infrared realm, chalcogenide glasses stand out as exceptional contenders for mid-infrared supercontinuum generation. Chalcogenide glasses consist of elements in group VI of the periodic table such as S, Se, and Te (called chalcogens) combined with network forming elements including Si, As, Ge, P, and Sb.

This project report aims at elucidating the various dispersion and nonlinear phenomena that lead to the generation of supercontinuum spectra. Further, as the prime objective of the project, a $Ge_{11.5}As_{24}Se_{64.5}$ based microstructured optical fiber is designed and modelled for supercontinuum generation using ‘MATLAB’ and the finite element mode-solver ‘COMSOL Multiphysics’. The simulations performed suggest that the proposed Ch-MOF possesses a high non linearity of 1001 W^{-1}/km and produces a broadband SC spectrum spanning from 1.4 μm to 16 μm at a pump wavelength of 3.1 μm with optical pulses having 4 kW peak power and 50 fs pulse width using only 20 mm of the fiber.

ACKNOWLEDGEMENT

First and foremost, I would like to express my sincere gratitude to my project supervisor, Dr. Ajeet Kumar, for his invaluable guidance, motivation and support throughout the extent of the project. I have benefitted immensely from his wealth of knowledge.

I am also grateful to Ms. Pooja Chauhan for helping me at all stages of my project work.

I extend my gratitude to my university, Delhi Technological University (formerly Delhi College of Engineering) for giving me the opportunity to undertake this project.

This opportunity will be a significant milestone in my career progression and i will strive to utilize the gained skills and knowledge in the best possible way.

Ankit Sharma
2K17/MOC/03
M.Tech MOC

CONTENTS

TABLE OF CONTENTS

LIST OF TABLES

LIST OF FIGURES

LIST OF SYMBOLS AND ABBREVIATIONS

Symbol/Abbreviation	Meaning/Expansion
A	Pulse Amplitude
A_{eff}	Effective Mode Area
c	Speed of Light
Ch	Chalcogenide
D	Dispersion Parameter
FEM	Finite Element Method
FWM	Four Wave Mixing
GNLSE	Generalized Nonlinear Schrödinger Equation
GVD	Group Velocity Dispersion
HNLF	Highly Nonlinear Fiber
MOF	Microstructured optical fiber
n_2	Nonlinear Refractive Index
n_{eff}	Effective Refractive Index
$n(\omega)$	Refractive Index
NLO	Nonlinear Optics
PCF	Photonic Crystal Fiber
PML	Perfectly Matched Layer
SBS	Scattering
SCG	Supercontinuum Generation
SPM	Self-Phase Modulation
SRS	Stimulated Raman Scattering
TIR	Total Internal Reflection

V	V- Parameter
v_g	Group Velocity
XPM	Cross Phase Modulation
ZDWL	Zero Dispersion Wavelength
α	Attenuation Constant
β	Mode Propagation Constant
β_1	First Order Dispersion Parameter
β_2	GVD Parameter
γ	Nonlinear Parameter/ Nonlinearity
Δ	Numerical Aperture
ϵ_0	Permittivity of Free Space
λ	Wavelength
μ_0	Vacuum Permeability
π	Pi
φ	Phase Shift
χ	Dielectric Susceptibility
ω	Carrier Frequency
ω_0	Central Carrier Frequency

Chapter 1

INTRODUCTION

This introductory chapter is envisioned to explicate the diverse characteristics of an optical fiber that are essential in order to have a better appreciation of the field of nonlinear optics and associated aspects which separate it from linear optics. It incorporates various sections providing a historical outlook on the developments made in the field of fiber optics and design features of a simple optical fiber which provide an outline of the various linear and nonlinear phenomena in the fiber. The interplay of the two aforestated phenomena, result in 'Supercontinuum Generation'- a broadband spectrum generated from ultra- short optical pulses. This whole literature review proves quite beneficial in designing and modelling a microstructured optical fiber to generate broadband supercontinuum spectra, which is the prime objective of this project.

1.1 LINEAR AND NONLINEAR OPTICS

Linear fiber optics deals with the propagation of an optical signal through a medium when the medium properties remain invariant with time. But, if the propagating signal itself causes a variation in the medium characteristics, the situation is dealt under the realm of nonlinear fiber optics. Nonlinear fiber optics is a more modern phenomenon which deals with the nonlinear effects that occur in a medium as the optical signal propagates through the medium. In a linear media, the dielectric polarization P varies linearly with the light's electric field E whereas in nonlinear media the two vector quantities exhibit a nonlinear relationship. This can be seen in figure 1.1.

Linearity or nonlinearity is not a characteristic of the light but rather a property of the medium through which the light propagates. When the propagation of an optical field through a medium alters the properties of the medium thereby, modifying another optical field or even the original field itself, such a field of study forms the branch of 'Nonlinear Optics (NLO)'. There are various properties which differentiate a linear optical medium from a nonlinear one.

Figure 1.1: Relationship between the electric field *E* vector and polarization *P* vector (a) in a linear medium and (b) in a nonlinear medium [33].

The properties of a linear optical medium are numerated as under:

(a) While propagating through a medium, the light intensity has no bearing on the optical properties, such as the refractive index and the absorption coefficient.

(b) The principle of superposition holds.

(c) As the light traverses the medium, its frequency remains unaltered during the process.

(d) No interaction takes place among the light beams in the same region of a linear optical medium i.e. light cannot control light.

However, in the case of a nonlinear medium, following are the observations that exemplify its properties:

(a) Optical properties such as the refractive index and the absorption coefficient depend upon the light intensity traversing through the medium.

(b) The principle of superposition doesn't hold.

(c) On passing through a nonlinear medium, a change in frequency can be incorporated by the light beam.

(d) Light beams can interact in a nonlinear medium i.e. light can control light.

1.2 HISTORICAL PERSPECTIVE

In order to identify a medium to propagate light over considerable distances for communication purpose, scientists preferred to choose glass since it was already being

employed in various optical experiments. However, at that time, the glass that was used for such experiments was found to have a very high loss figure in the range of 1000 dB/Km. Subsequently, investigations revealed that this high loss was not attributed by the glass molecules but was due to the presence of impurities in the glass that remained in it during its manufacture, leading to the high loss of optical energy propagating through it. This instigated various refinements in the existing manufacturing processes and consequently, scientists were successful in fabricating glasses with a loss figure of only 20 dB/Km. This was taken to be a great success in those days since such a loss figure was quite appreciable when compared to coaxial cables which was the widely employed means for wide band communication. Later on, technologies improved gradually and highly purified glass came into existence which had a very low attenuation. Figure 1.2 depicts the various facets associated with the purification stages in the manufacture of glass.

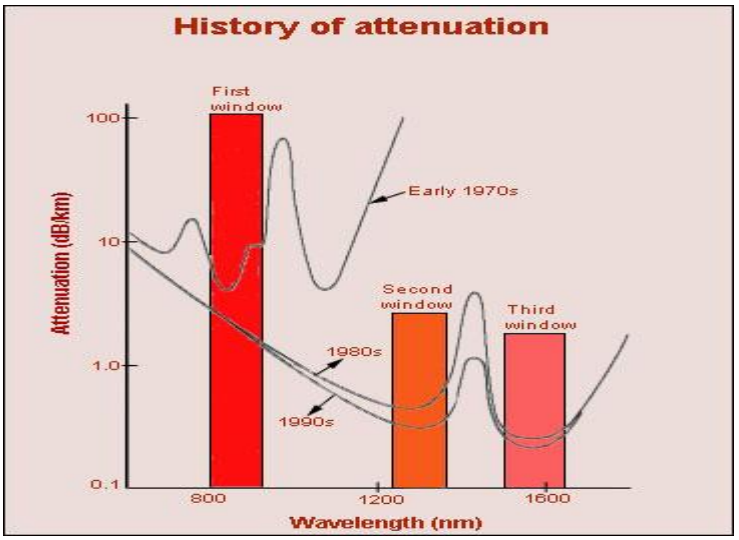

Figure 1.2: History of attenuation graph in the manufacture of glass [31].

As can be seen in figure 1.2, one can make out that owing to the drastic improvements in the fabrication of purified glass, the loss figures became negligibly small in comparison to other substitutes. It was rather a mere coincidence that during 1970s, when LASERs were fabricated using Gallium Arsenide (GaAs), which could emit light at 800nm wavelength, at that time scientists were successful in manufacturing glass having a minimum loss at around the same wavelength region. Hence, preliminary optical communications were initiated using the 800nm wavelength regime and is therefore, termed as the “First Window” of optical communication.

Subsequently, with additional refinements in the glass manufacturing process, it was possible develop glasses with a minimal loss at 1300nm and 1550nm regions. Specifically, these two wavelength regimes are known as the "Second Window" and "Third Window" of optical communication. Even though the second window of optical communication i.e. 1300nm regime had significant bandwidth but the same was compromised due to the higher associated losses. As a result, optical communications taking place in this window were largely affected from this higher loss, thereby, leading to the degradation of the communication system as the distances became substantially large. Presently, with the advent of optical amplifiers, which can directly amplify the light signals in optical domain, most of the optical communications are realized in the "Third Window" of optical communication i.e. 1550nm region.

Prior to the discovery of LASER and the fabrication of low loss silica fibers, all optical media was believed to exhibit only linear effects. However, with the generation of high intensity light beams through LASER and their propagation through low loss silica fibers enabled us to carry out various experiments to establish the nonlinear behaviour of optical media. Subsequently, various studies were carried out pertaining to different nonlinear phenomena such as self-phase modulation, cross phase modulation, Stimulated Raman Scattering (SRS), Stimulated Brillouin Scattering (SBS), four- wave mixing and optically induced birefringence in optical fibers.

In the year 1980, during an experiment light pulses were observed which didn't undergo any spectral or temporal change when propagated through the fiber. It was concluded that these pulses were basically produced owing to the interplay between nonlinear and dispersive phenomena taking place inside the fiber and were termed as 'optical solitons'. This was a remarkable discovery which paved the way for generation of ultrashort optical pulses.

During 1990s, optical amplifiers, fabricated using erbium doped silica optical fibers, came into existence which gave rise to new possibilities of amplifying optical signals directly in the optical domain without converting them first to electrical signals. This development added a new facet in the field of nonlinear fiber optics and transfigured the design of multichannel lightwave systems.

The year 1996 marked the development of new types of fibers whose dispersive and nonlinear properties could be tailored by the incorporation of various changes possible in the fiber structure. These fibers were termed as the photonic crystal

fibers, holey fibers and microstructured fibers. Owing to the smaller core region, these fibers were capable of displaying enhanced nonlinear effects in comparison to the existing fibers. After the year 2000 [27], nonlinear effects of stimulated Raman scattering and four-wave mixing enabled the fabrication of fiber-based amplifiers which could operate in any spectral region with absolutely no doping. This amalgamation led to the study of more nonlinear phenomena such as that of supercontinuum generation i.e. the significant spectrum broadening of high intensity laser pulses while traversing through a highly nonlinear medium.

All the aforestated developments over the last few decades have played a pivotal role in the growth of the field of nonlinear optics and it can be said on a firm basis that the same will nurture at a much faster pace in the times to come.

1.3 OPTICAL FIBER

Basically, an optical fiber comprises of a central region called the 'core' fabricated using a solid glass rod encapsulated in another coaxial glass shell called the 'cladding'. Optical signals propagate through the core which has a higher refractive index as compared to the cladding. Figure 1.3 shows the cross-section constructional details of an optical fiber.

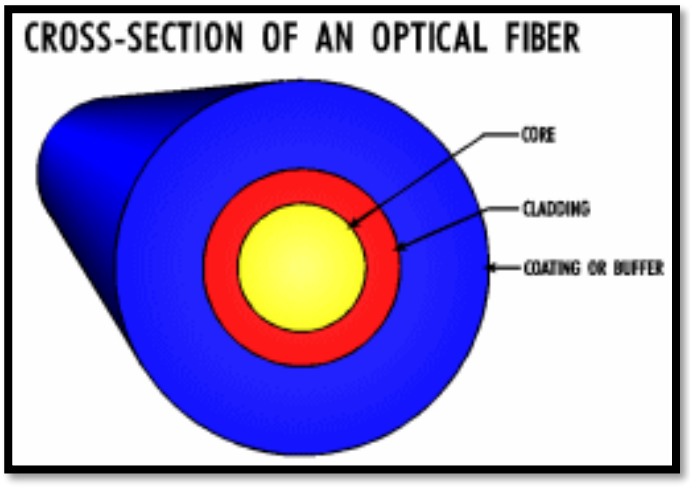

Figure 1.3: Cross sectional view of an optical fiber [31].

An optical fiber is a very thin glass rod with a cladding diameter of the order of 125 μm and a core diameter even smaller than that, which makes it quite fragile. Hence, jacketing layers called the buffer coating are provided encapsulating this core-cladding arrangement in order to ensure sufficient mechanical strength.

1.3.1 Guiding Mechanism in Optical Fibers

Figure 1.4 depicts the refractive index profile of a standard step-index fiber along with a graded index fiber and a photonic crystal fiber. In a step-index fiber, the core has a relatively higher refractive index as compared to the cladding. The higher refractive index of the core is ensured by either doping the core with germanium oxide or by doping the cladding with fluoride to lower its refractive index, or indeed a combination of the two. The phenomenon responsible for guiding the optical signals inside an optical fiber is called the Total Internal Reflection (TIR) of light that takes place at the interface between the core and cladding.

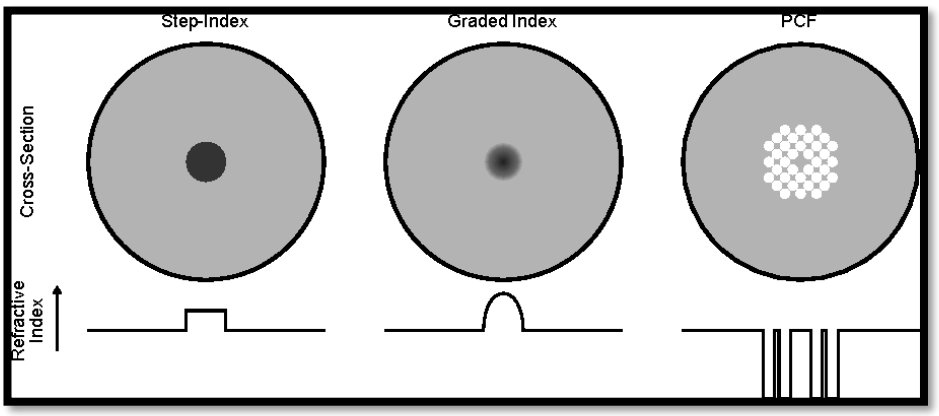

Figure 1.4: Refractive index profiles of different types of fiber [36].

Apart from the normal step index fiber, there are other diverse fiber geometries which are being employed to enhance the nonlinearity of the fiber, or to tailor the fiber dispersive properties. Graded-index fiber (also shown in Figure 1.4) exhibit parabolic index profiles across the core region. In photonic crystal fibers, a subset of microstructured fibers, an array of airholes is incorporated so as to realize a relative refractive index difference between the core and cladding regions. Solid core PCFs are usually fabricated using pure silica with air holes arranged in a regular pattern around the core and running throughout the fiber length (shown in figure 1.4). Such an arrangement ensures a strong confinement of light in between the core and cladding regions due to a rather large refractive index difference between them. Owing to their high nonlinearity and the ability to tailor the geometry of the PCFs to achieve dispersion curves impossible in conventional fiber, PCF has found vital applications in supercontinuum generation.

Fundamentally, the relative core-cladding index difference or the numerical aperture of the fiber and the V- parameter are two parameters that characterize an optical fiber.

Numerical Aperture basically signifies the light gathering effectiveness of an optical fiber. Higher the value of numerical aperture, more efficient is the fiber. The numerical aperture of the fiber can be defined as:

$$\Delta = \frac{n_1 - n_2}{n_1} \tag{1.1}$$

where n_1 is the refractive index of the core and n_2 is the refractive index of the cladding.

The V- parameter is a dimensionless number that determines how many modes a fiber can support. It is defined as:

$$v = k_0 a \sqrt{(n_1^2 - n_2^2)} \tag{1.2}$$

where $k_0 = 2\pi/\lambda$, where 'a' is the core radius and λ is the wavelength of light.

1.4 ORGANISATION OF CHAPTERS

The second chapter discusses the types of fiber dispersion which affect the propagation of an optical wave in an optical fiber. These include chromatic dispersion (which is basically the material dispersion), waveguide dispersion and polarization mode dispersion. The normal and anomalous dispersion regime with respect to the GVD parameter is also discussed. Chapter Three discusses the various nonlinear effects that are common to silica glasses and other media in general. The wave equation and pulse propagation in nonlinear fibers is then discussed in Chapter Four. Certain types of nonlinear fibers such as holey fibers and photonic crystal fibers are discussed. Chapter Five introduces the topic of supercontinuum generation comprising of certain results previously obtained in bulk, silica-based and photonic crystal fibers. The final chapter, Chapter Six, deals with the designing and modelling of the microstructured optical fiber making use of all the literature that has been studied in the previous chapters.

Chapter 2

SIGNAL DISTORTION IN OPTICAL FIBERS

In the process of transmitting a light signal through an optical fiber, it gets distorted owing to two phenomena, namely - 'Dispersion' and 'Attenuation'. Various constituents of each phenomenon that result in the distortion of signal in the optical fiber are depicted in figure 2.1:

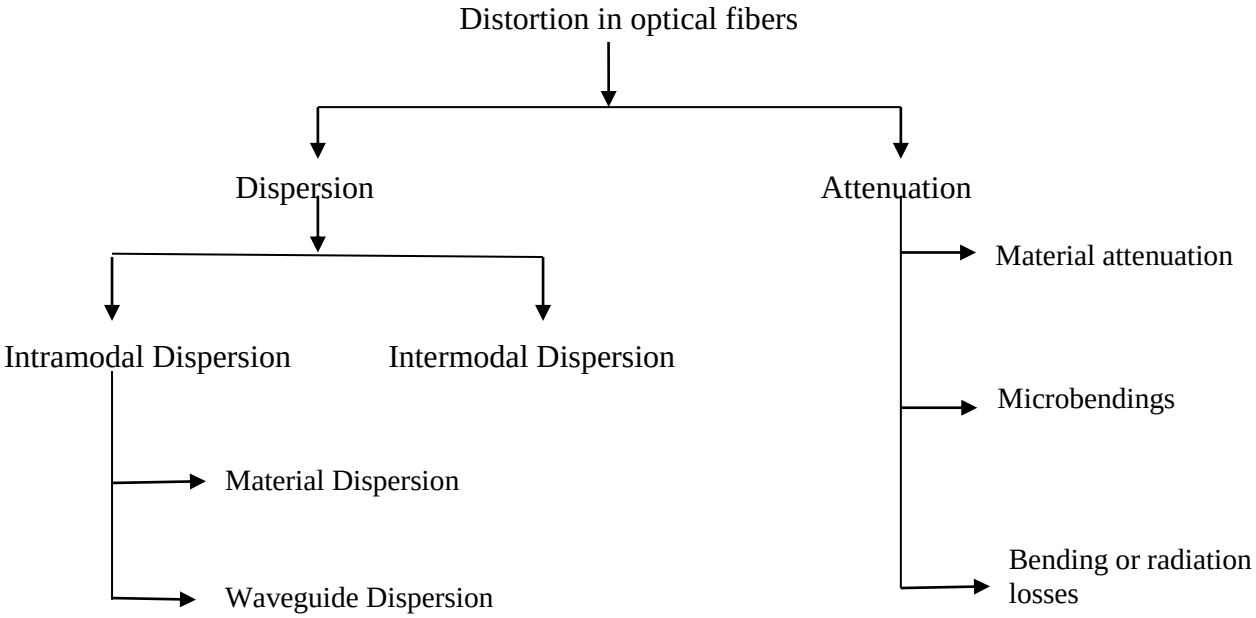

Figure 2.1: Constituents causing distortion in optical fibers [31].

2.1 SIGNAL ATTENUATION

Attenuation in optical fibers primarily signifies the loss of optical power associated with an optical signal as it propagates through the fiber. Let P_0 denotes the power injected into a fiber having length L, then the power transmitted (P_T) by the fiber is governed by the following expression [4]:

$$P_T = P_O \exp(-\alpha L) \tag{2.1}$$

where α is called 'Attenuation Constant' which represents the total losses that the fiber suffers from all sources. It is measured in units of dB/km.

The various mechanisms/factors responsible for attenuating a signal traversing through an optical fiber are: (1) Loss due to the intrinsic nature of the fiber material. (2) As a result of micro irregularities leading to the scattering of signal inside the fiber. (3) Micro-bending losses and, (4) Radiation/bending losses on the fiber. The first two losses are due to inherent properties of glass and hence, would always exist in the optical fiber even in the ideal condition when the fiber is not laid into the system. However, the last two losses don't arise due to the intrinsic characteristics of glass. These losses are basically the outcome of deformations produced in the fiber while laying it for various applications.

2.1.1 Material Loss

Various impurities present in glass used for fabricating optical fibers lead to material loss. Despite the finest cleansing and purifying processes, different impurities such as Al, Co, Ni, Fe are always available in the glass used for manufacturing optical fibers. In addition, some water molecules remain inside glass even after the glass has been carefully purified. Further, if glass is exposed to the atmosphere for extended time periods, water molecules may also get diffused into glass directly from the atmosphere. The presence of these water molecules leads to yet another absorptive loss which causes absorption peaks in the loss profile of glass.

2.1.2 Scattering Loss

During the fabrication of optical fiber, some imperfections termed as 'micro-centres' are formed inside the optical fibers having dimensions of the order of λ^{-4}. As a result of these micro-centers, scattering of light takes place inside the optical fibers, thereby attenuating the light signal. Since, practically it is not feasible to get the optical fiber cables aligned in perfectly straight lines for communication; hence, some of the micro-centers remain here and there which lead to spurious leakage of light energy leading to the loss of optical energy.

2.1.3 Micro-Bending Losses

During the commissioning of an optical fiber for various applications, the same gets constricted against an uneven surface leading to smaller scale twisting, termed as micro-bending depicted in figure 2.2. As a result of these microbends, axial distortions occur inside the fiber. We know that the phenomenon of total internal reflection (TIR) is responsible for guiding the light inside an optical fiber which takes place at the instant when the light rays at the core cladding boundary have an angle of incidence greater than the critical angle at the boundary. Formation of these microbends leads to deviation in the position of the local normal w.r.t the core-cladding boundary thereby, restricting the rays to have a higher angle of incidence than the critical angle and thus, hampering the phenomenon of TIR. As a result, the rays will be leaked out, resulting in the enhancement of the fiber loss by 0.1-0.2 dB/Km.

2.1.4 Radiation or Bending Loss

Similar to the case of micro-bends, optical fibers may undergo a slow bend while commissioning of the fibers for various applications. Although the bending is on micron scale in the case of micro-bend, the same grows to the cm range in case of a slow bend. When fibers are laid in the form of large arcs or 'macro-bends', it gives rise to another phenomenon referred to as 'Radiation loss' which causes loss of light energy, thereby, leading to attenuation of the optical signal within the optical fiber. Every bent fiber gets affected with this radiation loss, no matter how moderate the bend is.

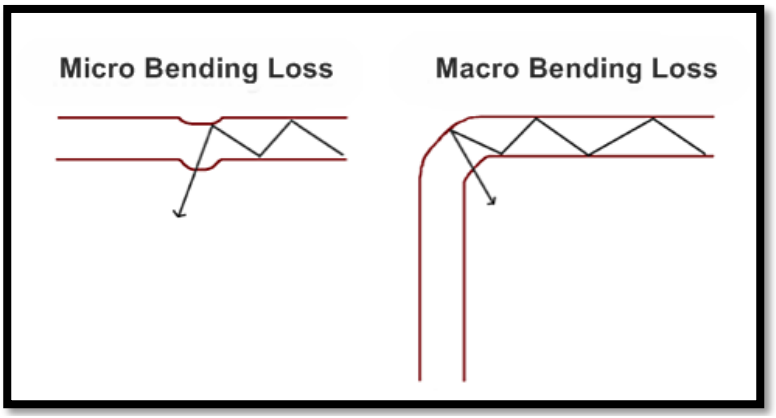

Figure 2.2: Micro and Macro bending in optical fibers [24].

2.2 CHROMATIC DISPERSION

In the field of optics, dispersion refers to the phenomenon wherein the velocity with which a light wave travels relies upon its associated frequency. The term ‘Dispersive media’ is usually employed for media exhibiting such a feature. The most widely recognized case of dispersion is perhaps a rainbow, wherein the said phenomenon leads to the spatial split-up of white light into segments of various wavelengths (various hues). However, both digital and analog transmissions over an optical fiber get distorted as a result of dispersion and consequently, the optimum conceivable bandwidth also gets restricted that would have been achieved with a specific optical fiber. Dispersion, at times, is referred to as chromatic dispersion in order to underline its wavelength-reliant nature.

As a result of dispersion, the light pulses propagating inside the fiber get broadening effect during their course of travel within the fiber. Consequently, each pulse widens and merges with its adjacent pulses, ultimately becoming inseparable at the receiver. This impact is termed as ‘Intersymbol Interference’, as illustrated in figure 2.3:

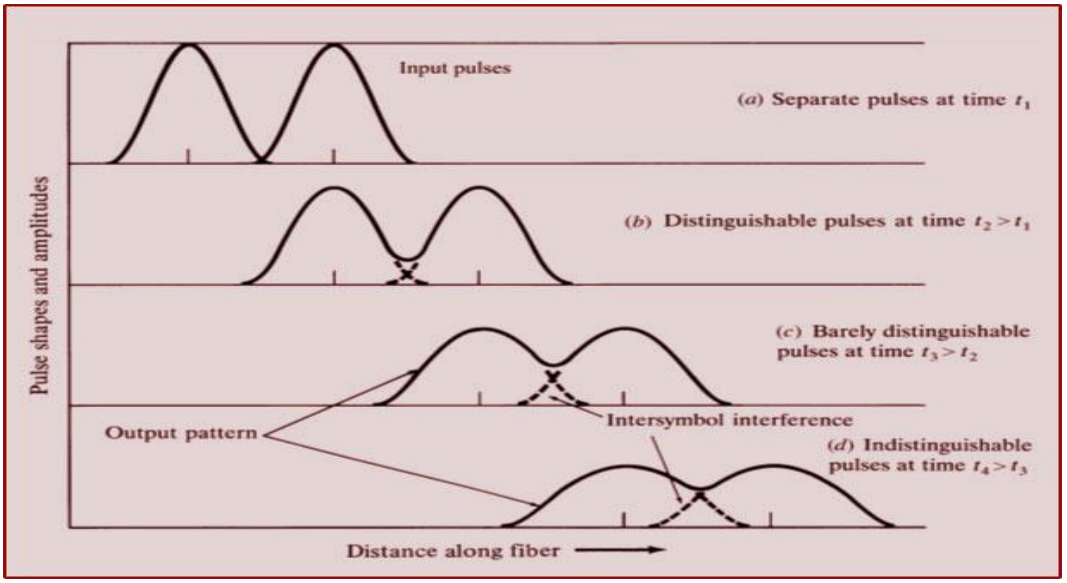

Figure 2.3: Pulse broadening in an optical fiber [31].

Chromatic dispersion can be said to be originating fundamentally from the fact that for different frequencies, there is a variation in the manner in which an electromagnetic wave propagating through the medium interacts with its bound electrons. Basically, chromatic dispersion arises due to the distinctive resonance frequencies at which electromagnetic radiation is absorbed by a material. This absorption takes place due to the oscillations of the bound electrons through their interaction with the incident electromagnetic wave.

This causes a variation in the material's response and hence, a variation in the refractive index of the material [1]. Chromatic dispersion is thus, the variation of the refractive index of the material with the frequency of operation of the incident electromagnetic wave.

For frequencies much far away from the material's resonant frequencies, the refractive index is approximated using the Sellmeier equation. The Sellmeier equation builds up an exact correlation between the refractive index and wavelength for a specific transparent medium. In its standard form, the said equation is given as [4]:

$$n^2(\omega) = 1 + \sum_{j=1}^{m} \frac{B_j \omega_j^2}{\omega_j^2 - \omega^2} \tag{2.2}$$

where B_j is the strength of j^{th} resonance and ω_j is the resonance frequency. The parameters B_j and ω_j are empirical values which depend on the constituents of the core and are obtained experimentally.

2.2.1 Intramodal Dispersion

Intramodal dispersion occurs since optical sources have a finite spectral width. This means that optical sources don't emanate only a single frequency but a range of frequencies. In case of a LASER, it corresponds to only a small proportion of the center frequency, while for an LED it corresponds to a considerable percentage. As a result, delay differences may arise among the various spectral components during the propagation of the transmitted signal, resulting in the broadening of each transmitted mode and hence, causing Intramodal dispersion.

2.2.2 Material Dispersion

The material dispersion arises due to the intrinsic property of a material. Glass is a dispersive medium i.e. its refractive index varies in accordance with the wavelength of the propagating optical pulse.

Now, we know that,

$$n = c/v \tag{2.3}$$

where n denotes the refractive index, c denotes the speed of light in vacuum and v is the speed at which the optical pulse traverses through the material.

Hence, as per the above expression, optical pulses having various wavelengths propagate through a glass fiber with varying speeds since glass is a dispersive medium. This type of dispersion mechanism is termed as material dispersion, owing to the fact that it primarily arises due to the properties inherent in the fiber material. The following expression signifies material dispersion:

$$D_{mat} = -\frac{\lambda}{c}\frac{d^2n}{d\lambda^2} \tag{2.4}$$

where c = Velocity of light, λ= wavelength, $\frac{d^2n}{d\lambda^2}$ = Second order derivative of refractive index w.r.t. wavelength.

2.2.3 Waveguide Dispersion

A single mode fiber exhibits waveguide dispersion as a result of the relative refractive index variation between the core and the cladding. As a light pulse propagates through the fiber, optical energy traverses at somewhat varying velocities in the core and cladding owing to their distinct indices of refraction. This finally, results in a “drag” effect between the segments of power of the optical pulse in the core and the cladding regions. However, by modifying the internal structures of the fiber, by altering parameters such as NA, core radius etc., waveguide dispersion can be significantly transformed.

2.2.4 Intermodal Dispersion

Multimode fibers exhibit intermodal dispersion mechanism. We know that a light pulse comprises of multiple modes. While propagating inside an optical fiber, each mode travels in a different direction and covers a different distance within the same time period. Consequently, the light pulse broadens since each mode travels through the fiber at varying speeds, hence causing dispersion.

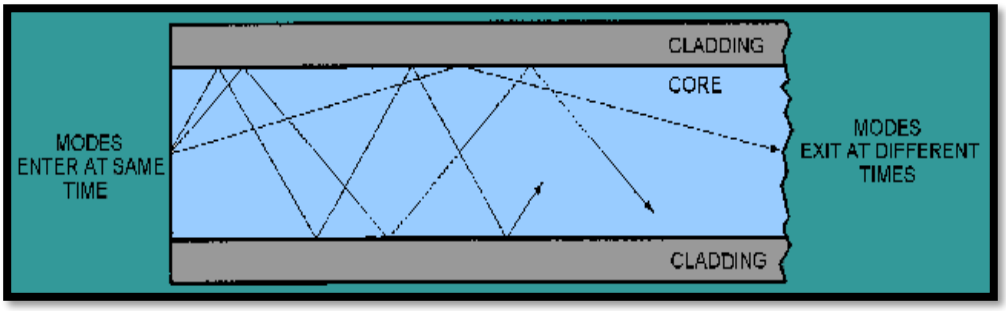

Figure 2.4: Intermodal dispersion in optical fibers [29].

2.2.5 Group Velocity Dispersion

As the refractive index is frequency dependent, pulses with considerable spectral width will be subjected to chromatic dispersion. This may be considered by expanding the mode-propagation constant β in a Taylor series about the pulse's central frequency ω [1,4]:

$$\beta(\omega) = \beta_0 + \beta_1(\omega - \omega_0) + \frac{1}{2!}\beta_2(\omega - \omega_0)^2 + \cdots \qquad (2.5)$$

where,

$$\beta_m(\omega) = \left(\frac{d^m\beta}{d\omega^m}\right)_{\omega = \omega_0} \qquad (m = 0,1,2 \ldots)$$

The first order term contains β_1, the inverse of the group velocity, v_g, of the pulse which is accountable for the overall delay on a pulse. The second order term contains β_2, the derivative of inverse group velocity with respect to frequency, and accounts for the variation in group velocity for different frequency components within the pulse, resulting in group-velocity dispersion (GVD).

GVD results in temporal broadening of an initially unchirped pulse as different frequency components travelling with varying velocities walk off with respect to each other. The GVD of a fiber at a given frequency is said to be normal when $\beta_2 > 0$ (group velocity decreasing with increasing optical frequency) or anomalous for $\beta_2 < 0$ (group velocity increasing with increasing optical frequency). The anomalous dispersion regime is often used to study nonlinear effects because optical solitons are supported by fibers only in this regime.

Optical soliton refers to a pulse that is broadened neither in the temporal domain nor the spectral domain when it propagates through a nonlinear dispersive medium. This occurs as a consequence of the interplay among the dispersive and various nonlinear phenomena present in the fiber, as depicted in figure 2.5.

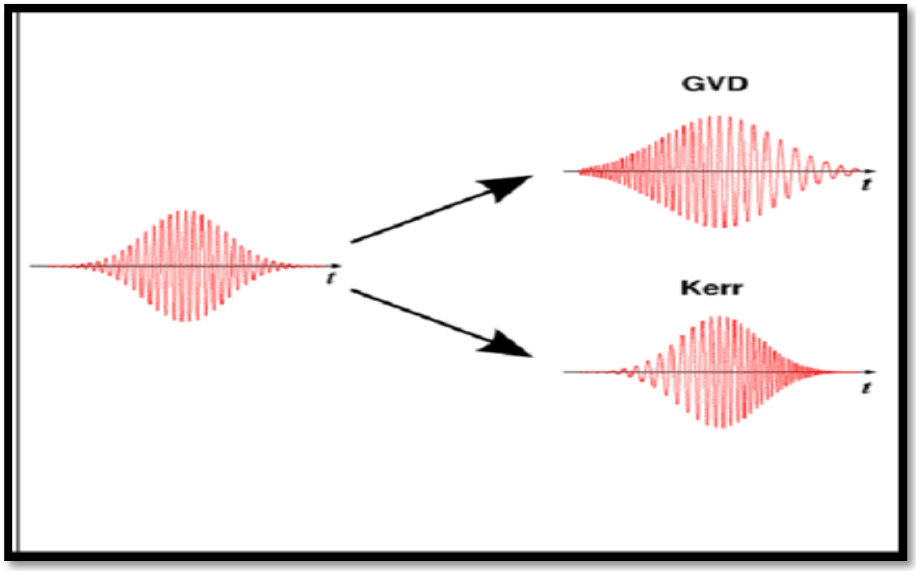

Figure2.5: Temporal broadening and chirping for an optical pulse in linear dispersive media due to GVD. Opposite chirping and no temporal broadening in an optical pulse in nonlinear non-dispersive media. Mutual compensation of the two phenomenon leads to the formation of an optical soliton in nonlinear dispersive media [1].

The wavelength corresponding to a value of $\beta_2 = 0$ is called the zero-dispersion wavelength (ZDWL). Also, the dispersion parameter 'D' defined as $d\beta_1/d\lambda$. It can be related to β_2 and n as [4]:

$$D = \frac{d\beta_1}{d\lambda} = -\frac{2\pi c}{\lambda^2}\beta_2 = -\frac{\lambda}{c}\frac{d^2n}{d\lambda^2} \tag{2.6}$$

In the absence of nonlinear effects, pulse broadening due to GVD can significantly hamper optical communication systems. However, the amalgamation of dispersion and nonlinearity, in the nonlinear regime, can lead to an overall positive effect, making the material apposite for multifarious applications such as supercontinuum generation (SCG).

2.2.6 Polarization Mode Dispersion

Polarization mode dispersion (PMD) is a type of intermodal dispersion which arises as a result of arbitrary imperfections in the structure of an optical fiber. Due to the random asymmetries in the fiber structure, two distinct polarizations of an optical pulse, which usually propagate at identical speeds, travel at varying speeds through the fiber. This effect leads to spreading of the pulse thereby, causing it to merge with other pulses or undergo a shape change sufficient to make it imperceptible at the receiver end. This ultimately limits the rate at which data can be transmitted over a fiber.

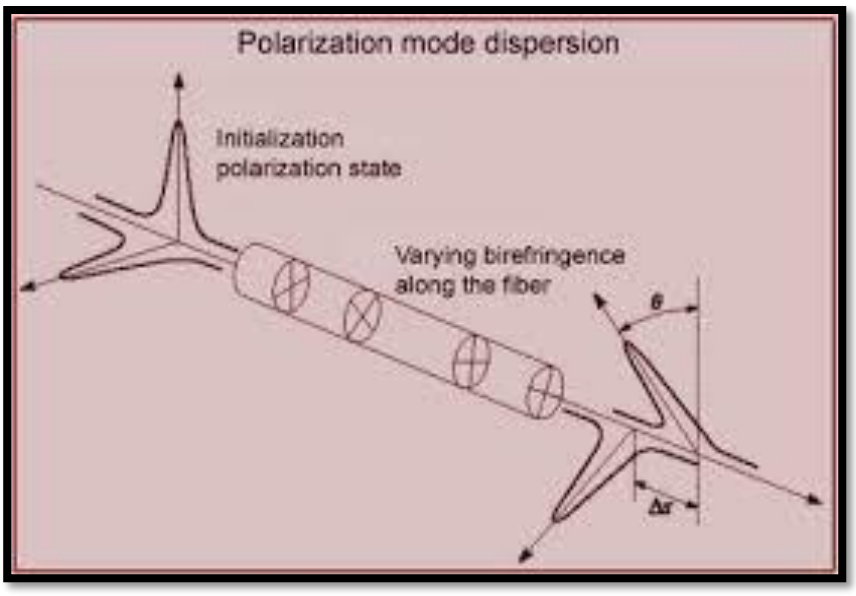

Figure 2.6: Polarization mode dispersion in optical fibers [31].

Figure 2.6 shows the propagation of an optical pulse through an optical fiber.

Subsequently, when the pulse gets affected as a result of PMD, the polarized energy splits up by some time, after some distance as shown in figure 2.6. This time span is termed as differential group delay (DGD) and is an essential parameter in the measurement of PMD.

Consequently, in case the DGD is severe, it would be rather impossible for the receiver to precisely decipher the optical pulse, thereby leading to bit errors.

Random imperfections, such as slightly out of shape fiber core, in the fiber structure are the primary cause of PMD. Such an asymmetry may result in the fiber during the fabrication process or due to mechanical stress during the commissioning of the fiber for various applications.

Chapter 3

NONLINEAR FIBER OPTICS

3.1 NONLINEAR OPTICAL MEDIA

When the medium properties don't change with time as the transmitted optical signal propagates through the medium, the situation is dealt under 'Linear Fiber Optics'. However, if the variation in medium characteristics is caused by the signal traversing through it, the situation is dealt under 'Nonlinear Fiber Optics'. Nonlinear fiber optics refers to the branch of optics which deals with the nonlinear effects that emerge in a medium as the optical signal propagates through the medium.

In case of a linear dielectric medium, there exists a linear relationship between the polarization density vector **P** and the electric field vector **E** and can be given by the simple relation [1]:

$$\mathbf{P} = \epsilon_0 \chi \mathbf{E} \tag{3.1}$$

where χ is the linear dielectric susceptibility and ϵ_0 is the permittivity of free space.

When a dielectric medium is placed in an electric field, it becomes polarized and the susceptibility of the medium is a measure of the same. In general, the first order susceptibility is considered as the dielectric constant of the medium, overlooking the influence of the higher order terms. However, this is only an approximation which does not hold for strong electric fields i.e. light of high intensity. In practice, when an intense electromagnetic field is applied, dielectric materials like optical fibers exhibit a nonlinear response. This nonlinear response can be accredited to the non-harmonic motion of the material's bound electrons on the application of an electric field. Since light intensity produced by sources like LASERs is very high, hence, we have to take into account the contribution of higher order terms correlated to the medium's polarization.

The induced polarization, **P**, in a dielectric medium placed in an electric field **E** is given by the expression [1,4]:

$$\mathbf{P} = \epsilon_0\{\chi^1 \cdot \mathbf{E} + \chi^2 : \mathbf{EE} + \chi^3 \vdots \mathbf{EEE} + \cdots\} \tag{3.2}$$

The above expression correlating **P** and **E** is basically linear for small values of **E**, differing from linearity with an increase in the value of **E** (typically 10^5 to 10^8 V/m). In general, the first term on the RHS is known as the dominant term and it contributes to the dielectric constant of the medium. The effects of this tensor are incorporated in terms of the refractive index *n* and the attenuation coefficient α. The second term in the RHS which is a second order term is dependent on the electric field and contributes to nonlinear effects such as second harmonic generation and sum frequency generation. However, in case of a centrosymmetric molecule such as glass (SiO_2), the value of χ^2 is negligibly small. Consequently, optical fibers generally do not display second order nonlinear effects. But it is the third term in the above expression, containing χ^3, that contributes to the nonlinear effects in SiO_2.

At the fundamental level, it is only the third order susceptibility χ^3 which is accountable for the lowest order nonlinear effects arising from nonlinear phenomena such as third harmonic generation, four wave mixing and nonlinear refraction, since the second order susceptibility χ^2 is generally zero for silica based optical fibers. But, since it is essential to achieve phase matching (which does not usually happen) for the said phenomena to occur effectively in optical fibers, hence, majority of the nonlinear phenomena in optical fibers initiate from nonlinear refraction wherein the refractive index of the material in the fiber depends on the intensity of EM wave, as represented by the following expression [4]:

$$\tilde{n}(\omega, I) = n(\omega) + n_2 I = n + \bar{n}_2 |\mathbf{E}|^2 \tag{3.3}$$

where $n(\omega)$ is the linear refractive index and $\bar{n}_2|\boldsymbol{E}|^2$ is the term contributing to the nonlinearity in the refractive index. The term n_2 is a medium dependent quantity, called the nonlinearity coefficient and is associated with the third order susceptibility χ^3 of the material.

As a result of the reliance of refractive index on the intensity of an optical pulse, multiple remarkable nonlinear effects come into play, out of which self-phase modulation (SPM) and cross phase modulation (XPM) are the most common ones.

These nonlinear phenomena that are determined by the third-order susceptibility χ^3 are termed as elastic in nature i.e. no exchange of energy takes place amid the EM field and the dielectric material during their interaction with each other. This phenomenon is termed as 'Elastic Scattering'. On the other hand, if the optical field relocates a part of its energy to the dielectric medium, then the phenomenon is called as 'Stimulated Inelastic Scattering'. Essential nonlinear phenomena in optical fibers that fall into this group include stimulated Raman scattering and stimulated Brillouin scattering.

3.2 NONLINEAR EFFECTS AS AN OUTCOME OF KERR EFFECT

3.2.1 Self Phase Modulation

Self-Phase Modulation (SPM) occurs as a result of Kerr effect. Also known as quadratic electro-optic effect, the Kerr effect is a phenomenon observed in nonlinear optic materials wherein the material's refractive index gets modified upon the application of an electric field as represented in equation (3.3).

While the high intensity segments of the optical pulse come across a high refractive index of the fiber, a lower refractive index is encountered by the lower intensity segments. Due to varying refractive index, the pulse experiences a self-induced phase shift. This phase change of the optical field is given as[4]:

$$\varphi = \tilde{n}\, k_0 L = (n + \bar{n}_2 |\mathbf{E}|^2) k_0 L \tag{3.4}$$

where $k_0 = 2\pi/L$ and L denotes the fiber length. The intensity reliant nonlinear phase shift $\varphi_{NL} = n_2 |\mathbf{E}|^2 k_0 L$ is due to SPM. Although, the nonlinear phase shift increases with the fiber length L, as represented in equation (3.4), there is no change in the shape of the pulse during this phase shift.

Now, the effective length L_{eff} for a fiber of length L can be defined as [4]:

$$L_{eff} = \frac{[1 - \exp(-\alpha L)]}{\alpha} \tag{3.5}$$

where α accounts for the fiber losses. Here, L_{eff} denotes the effective length which is smaller in comparison to L since it accounts for the fiber losses. Now, if there are no fiber losses (α = 0), and L_{eff}= L then the maximum phase shift is then given as [4]:

$$\varphi_{max} = \frac{L_{eff}}{L} = \gamma P_0 L_{eff} \tag{3.6}$$

where γ denotes the nonlinear parameter correlated to the nonlinear Kerr coefficient n_2 by Equation (4.17) and P_0 is the peak power. From Equation (3.6), we can define the nonlinear length L_{NL} as the effective propagation distance at which $\varphi_{max} = 1$.

Spectrum broadening of ultra-short pulses propagating through the fiber is primarily caused by self-phase modulation in such a way that the temporal shape remains unchanged but it results in frequency chirping of the pulse.

Frequency chirping is fundamentally comprehended as the time reliance of instantaneous frequency. In particular, an up-chirp (down-chirp) implies that the instantaneous frequency rises (decreases) with time. Now, this chirp, introduced as a result of self-phase modulation, increases in magnitude with propagated distance. This gives rise to the formation of novel frequency components continuously as the pulse traverses through the fiber, thereby leading to the spectral broadening of ultra-short pulses propagating through the fiber.

3.2.2 Cross Phase Modulation

When two optical pulses undergo concurrent propagation inside an optical fiber with different velocities then the pulse with higher speed surpasses the pulse traversing with lower speed. During this action, the overlap between the two pulses takes place which gives rise to the phenomenon of cross phase modulation (XPM).

However, as soon as the faster pulse completely bypasses the pulse with lower speed, the subsequent merging between the pulses becomes insignificant and the phenomenon of cross phase modulation vanishes. One can attribute this "walk-off" phenomenon to the variation in the respective group velocities of the pulses. Clearly, the merging between the two concurrent pulses would be considerable if there is a close interconnect between their group velocities leading to a higher cross phase modulation phenomenon. On the other hand, in case there is a significant variation in the respective group velocities, there would hardly be any overlapping between the pulses and XPM would not be excessively critical. Subsequently, this circumstance also will likewise look practically like self-phase modulation with the only variation that the phase modulation would be influenced by the existence of other signals as well. Clearly, we should choose a fiber which has an immense variation in the group velocity of the pulses so as to minimize overlapping between concurrent pulses thereby, weakening the XPM on the optical fiber. Basically, selecting an optical fiber with considerable dispersion will reduce the walk-off time significantly thereby, minimizing the intermingling of the two pulses. On the contrary, a dispersion flattened sort of optical fiber, wherein all the frequencies travel with practically equivalent group velocities leading to a higher nonlinear interaction among the optical pulses, will result in extensive cross phase modulation.

Therefore, some dispersion on the optical fiber is highly desirable in order to avoid the occurrence of cross phase modulation. Particularly, in a wavelength division multiplexed system, a dispersive optical fiber is necessary in order to curtail nonlinear interactions among various channels.

3.2.3 Four Wave Mixing

In a WDM framework with different channels, one significant nonlinear phenomenon is four-wave mixing. It is a sort of intermodulation effect which comes into picture when light of at least two distinct wavelengths propagates inside a fiber, resulting in the formation of a new wave.

To understand the effects of four wave mixing, let us consider three electric fields E_1, E_2, E_3 with three frequencies ω_1, ω_2, ω_3 and photon momenta k_1, k_2, k_3 respectively, incident on a medium with high third order susceptibility.

The nonlinear polarization in presence of these fields is given as:

$$P_{NL} = \epsilon_0 \chi^3 : E_1 E_2 E_3 \tag{3.7}$$

The interaction of three photons inside the material leads to the generation of a new photon such that the total energy and momentum is conserved. If the fourth photon has a frequency ω_4 and momentum k_4, then we must have:

$$\omega_4 = \omega_1 \pm \omega_2 \pm \omega_3$$
$$k_4 = k_1 \pm k_2 \pm k_3$$

Thus, novel fields at the frequencies $\omega_1 \pm \omega_2 \pm \omega_3$ are produced as a result of fiber's nonlinear susceptibility. This phenomenon is termed as 'Four-Wave Mixing' and is depicted in figure 3.1.

Now, when the channels are equally spaced in a WDM system i.e. $\omega_{2=}\, \omega_1 + \Delta\omega$ and $\omega_3 = \omega_1 + 2\Delta\omega$ and the new frequency generated is:

$$\omega_4 = \omega_1 - \omega_2 + \omega_3 = \omega_1 - (\omega_1 + \Delta\omega) + (\omega_1 + 2\Delta\omega) = \omega_2$$

This means that the two neighbouring channels of a WDM system exchange power with the middle channel. Hence, we can say that a cross talk is introduced between the WDM channels in the presence of four wave mixing.

From the above, it is clear that whereas Self-Phase Modulation (SPM) and Cross-Phase Modulation (XPM) effects are quite considerable for large data rate systems, the phenomenon of four-wave mixing doesn't depend on the bit rate but is significantly affected by the channel spacing and dispersion effects in the fiber. Thus, the consequence of Four-Wave Mixing must be taken into account for systems even with a moderate data rate in the event of using dispersion-shifted fibers and/or channels are closely spaced.

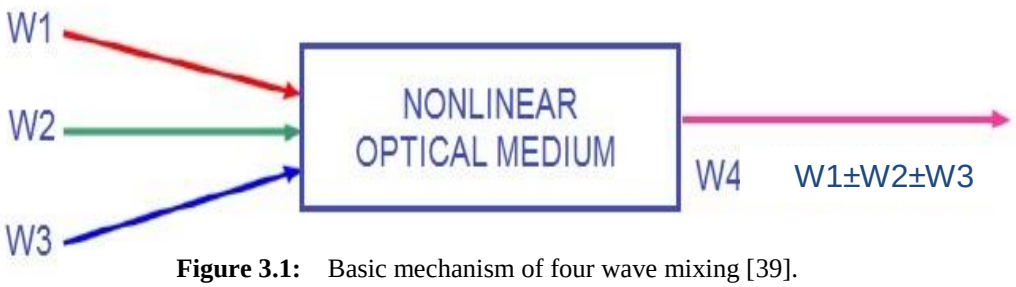

Figure 3.1: Basic mechanism of four wave mixing [39].

3.3 AS A RESULT OF INELASTIC SCATTERING

In the event that the optical field exchanges a portion of its energy to the dielectric medium, then what follows, is called as stimulated inelastic scattering. Raman scattering (SRS) and stimulated Brillouin scattering (SBS) are the two significant nonlinear phenomena which affect optical fibers that lie under this classification.

If the material medium atoms have a nonlinear polarization with a delayed response, caused by vibrations of the crystal lattice, it cannot be considered as a part of Kerr effect. The phenomena is termed as 'Raman Scattering' in case the said vibrations are related to optical phonons, otherwise, the effect is called Brillouin Scattering if these vibrations are related to acoustical phonons.

3.3.1 Stimulated Raman Scattering

At the point when optically flawless solids are exposed to monochromatic radiation of frequency ω_1, a significant part of the radiation surpasses them without any variation, however some portion of the radiation gets scattered.

Most of the scattered photons encompass the similar frequency and hence, wavelength like the incident photons i.e. they are elastically scattered, nonetheless, a little bit portion of light (approximately 1 in 10^7photons) gets scattered at distinctive frequencies as compared to the incident photons. The procedure prompting this inelastic scatter is called Raman Scattering which occurs as a result of transformation in the various energy regimes of a molecule.

If the spectrum of the scattered radiation is analyzed, it will be observed that in addition to the frequency ω_1 of the incident radiation, there will be pairs of new frequencies of the type $\omega_1 \pm \omega_m$. These novel frequencies are named as Raman lines or 'Bands' which jointly establish a Raman spectrum.

Now, bands of frequencies with magnitude lesser in comparison to the incident frequency i.e. $\omega_1 - \omega_m$ are called 'Stokes Bands' while bands of frequencies higher in comparison to the incident frequency i.e. $\omega_1 + \omega_m$ are called 'Anti Stokes Bands'. The energy-level diagram depicting various states in a Raman spectrum is shown in figure 3.2.

Raman scattering presents critical preferences for the examination of materials over other systematic methods, for example, X-raying them. Since Raman bands result directly from the molecular vibrations, which are very sensitive to changes in chemistry and structure of the material, it is possible to find out even the subtle changes in molecular environment.

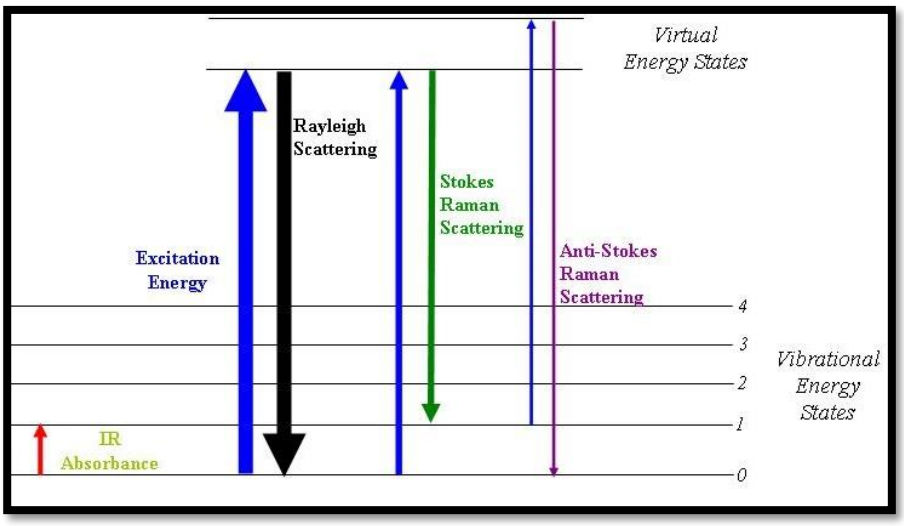

Figure 3.2: Energy-level diagram depicting various states in a Raman spectra [40].

3.3.2 Stimulated Brillouin Scattering

Certain materials have an affinity of getting compressed when an electric field is applied across them. This effect is termed as 'Electrostriction' and is the physical procedure behind the phenomena of Stimulated Brillouin Scattering.

Stimulated Brillouin Scattering (SBS) basically refers to a resonant nonlinear phenomenon that occurs in optical fibers due to the propagation of optical pulses having high intensity. It refers to the phenomenon in which the transmitted light is scattered back towards the input when the power pumped inside the fiber surpasses the threshold power level given by:

$$P_B = 4.4 \times 10^{-3} d^2 \lambda^2 \alpha_{dB} v \quad \text{watts} \tag{3.8}$$

where d and λ represent the fiber's core diameter and operating wavelength, α_{dB} represents the attenuation loss in dB/Km and v signifies the source bandwidth in GHz. The above expression stipulates the threshold power level which must be pumped inside a single mode optical fiber prior to the occurrence of SBS.

The basic mechanism of Stimulated Brillouin Scattering (SBS) is illustrated in figure 3.3. Due to electrostriction, the input signal called the pump wave generates an acoustic wave in the transmission medium (optical fiber). When the acoustic wave travels through the fiber, it instigates spatially changing intermittent local compressions and expansions which subsequently creates local increases and decreases in the index of refraction. This phenomenon is designated “Photoelastic effect” whose magnitude increments as the optical power increases.

On reaching the SBS threshold level, the incident optical power causes variation in the refractive index of the optical fiber that gets acoustically altered to a degree that results in the scattering of the incident wave and produces ‘Stokes Wave’ which traverses in a reverse direction to the incident wave.

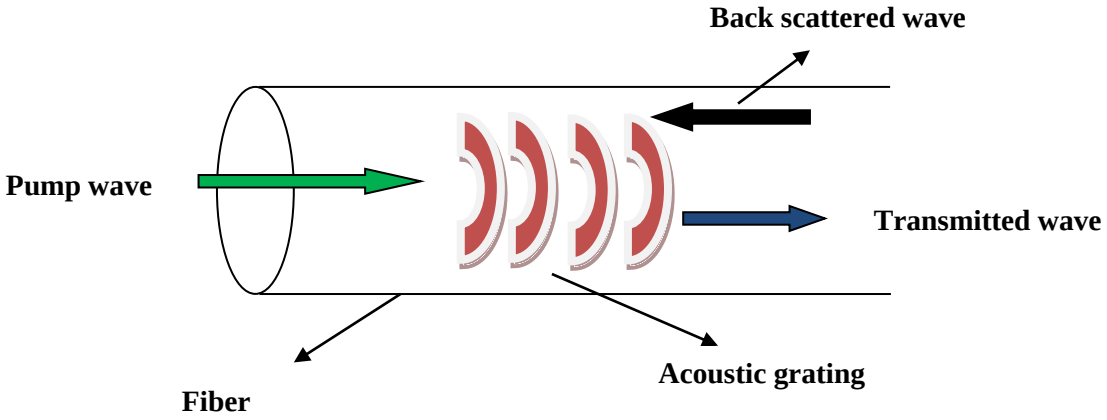

Figure 3.3: Basic SBS mechanism

Chapter 4

PULSE PROPAGATION IN NONLINEAR FIBERS

4.1 NONLINEAR WAVE EQUATION

To study the propagation of optical pulses within an optical fiber in the presence of nonlinear effects, the analysis requires to commence with basic Maxwell's equations. This is due to the fact that the Maxwell's equations themselves get modified in the presence of nonlinearity owing to the very simple notion that the displacement which is related to the polarization becomes nonlinear due to the presence of nonlinear term in the polarization as brought out by equation (3.2):

$$\nabla \times \mathbf{H} = \frac{\partial \mathbf{D}}{\partial \mathrm{t}} \tag{4.1}$$

$$\nabla \times \mathbf{E} = -\frac{\partial \mathbf{B}}{\partial \mathrm{t}} \tag{4.2}$$

$$\nabla . \mathbf{D} = 0 \tag{4.3}$$

$$\nabla . \mathbf{B} = 0 \tag{4.4}$$

In the above equations **E** and **H** represent the electric and magnetic field vectors, respectively, while **D** and **B** represent the corresponding electric and magnetic flux densities. Here, the current density vector **J = 0** and the charge density $\boldsymbol{\rho_f = 0}$, since in optical fibers there is an absence of free charges.

Now, since the displacement current density D is related to polarization as $\mathrm{D} = \boldsymbol{\epsilon_0 \mathbf{E} + \mathbf{P}}$, it is nonlinear due to the presence of nonlinearity in the polarization as shown in equation (3.2).

Further, in the presence of small electric fields, the higher order terms in the expression (3.2) can be ignored and thus, the polarization can be assumed to be linear. In this case, the displacement current density is then, given as:

$$\boldsymbol{D} = \boldsymbol{\epsilon_0}(\mathbf{1} + \boldsymbol{\chi^1})\boldsymbol{E} \tag{4.5}$$

Now, by taking the curl of equation (4.1) and using equation (4.2) along with expressions $\mathbf{D} = \boldsymbol{\epsilon_0}\mathbf{E} + \mathbf{P}$ and $\mathbf{B} = \mu_0\mathbf{H} + \mathbf{M}$, we can get the wave equation for the propagation of light inside an optical fiber using Maxwell's equations. Hence, we get:

$$\nabla \times \nabla \times \mathbf{E} = -\frac{\partial(\nabla \times \mathbf{B})}{\partial t} = -\mu_0 \frac{\partial^2 \mathbf{D}}{\partial t^2} \tag{4.6}$$

$$\nabla \times \nabla \times \mathbf{E} = -\frac{1}{c^2}\frac{\partial^2 \mathbf{E}}{\partial t^2} - \mu_0 \frac{\partial^2 \mathbf{P}}{\partial t^2} \tag{4.7}$$

using the relation $\boldsymbol{\epsilon_0\mu_0} = {}^{\mathbf{1}}/_{\boldsymbol{c^2}}$, where "c" is the speed of light in vacuum, where $\boldsymbol{\epsilon_0}$ and $\boldsymbol{\mu_0}$ represent the permittivity and permeability of free space. Substituting the value of $\mathbf{P}$ from expression (3.2), we get:

$$\mathbf{P} = \epsilon_0\{\chi^1 \cdot \mathbf{E} + \chi^3 \vdots \mathbf{EE}\} = \mathbf{P}_L + \mathbf{P}_{NL} \tag{4.8}$$

where,

$$\mathbf{P}_L = \epsilon_0\chi^1 \cdot \mathbf{E}; \qquad \text{Linear Part}$$

$$\mathbf{P}_{NL} = \epsilon_0\chi^3 \vdots \mathbf{EEE}; \qquad \text{Nonlinear part}$$

Since the second order susceptibility for glass is negligible, it is taken as zero in the above expression. Substituting these values in equation (4.7), we get:

$$\nabla(\nabla.\mathbf{E}) - \nabla^2\mathbf{E} = -\frac{1}{c^2}\frac{\partial^2 \mathbf{E}}{\partial t^2} - \mu_0\left\{\frac{\partial^2 \mathbf{P}_L}{\partial t^2} + \frac{\partial^2 \mathbf{P}_{NL}}{\partial t^2}\right\} \tag{4.9}$$

Since the dielectric constant is not spatially varying, we may use equations (4.3) and (4.4) and obtain the following wave equation:

$$\nabla^2\mathbf{E} - -\frac{1}{c^2}\frac{\partial^2\mathbf{E}}{\partial t^2} = \mu_0\left\{\frac{\partial^2\mathbf{P}_L}{\partial t^2} + \frac{\partial^2\mathbf{P}_{NL}}{\partial t^2}\right\} \tag{4.10}$$

In the above expression, the second term on the RHS is the nonlinear term that gets introduced due to integral nonlinearity of the medium. In case of linear medium properties, this term is absent and the equation reduces to the differential equation used in the analysis of linear optics.

4.2 PULSE PROPAGATION EQUATION

Starting with equation (4.7), the derivation of the propagation equation of optical pulses in a nonlinear dispersive medium such as fibers can be executed by making a few assumptions. First, the optical field is supposed to retain its polarization along the fiber length so that a scalar approach can be adopted and secondly, the nonlinear part of polarization is assumed to be a small perturbation to the linear part. It can be shown that pulses traversing inside an optical fiber with amplitude A and central frequency ω_0 will obey:

$$\frac{\partial A}{\partial z} + \beta_1\frac{\partial A}{\partial t} + i\frac{\beta_2}{2}\frac{\partial^2 A}{\partial t^2} + \frac{\alpha}{2}A = i\gamma(\omega_0)|A|^2A \tag{4.11}$$

where A is the pulse amplitude in V/m, β_2 is the second order coefficient in the expansion of the mode propagation constant , α is the attenuation coefficient which accounts for the losses inside the fiber and γ is defined as the nonlinearity parameter, given by:

$$\gamma = \frac{n_2\omega_0}{c\,A_{eff}} \tag{4.12}$$

Here, the quantity n_2 is termed as the nonlinear Kerr parameter measured in m^2/W. Consequently, γ has a unit of W^{-1}/m.

The term A_{eff} is the effective area of cross section of the optical fiber within which the light is confined and mathematically, it is expressed as:

$$A_{eff} = \frac{\left(\iint_{-\infty}^{\infty} |F(x,y)|^2 \, dxdy\right)^2}{\iint_{-\infty}^{\infty} |F(x,y)|^4 \, dxdy} \tag{4.13}$$

The quantity **F** is the transverse field distribution inside the optical fiber and knowing **F** enables us to determine the effective area A_{eff} within which the optical field is confined inside an optical fiber. Consequently, the nonlinearity parameter can thus, be determined from equation (4.12). Depending upon the core size of the optical fiber, field distribution, etc, the typical values of A_{eff} range between 1-100μm^2. Correspondingly, the typical values for γ range between 1-100 W^{-1}/Km.

Equation (4.11) elucidates the behaviour of evolution of the optical signal envelope with time as the signal propagates along the optical fiber. The said equation is correlated to the nonlinear Schrödinger (NLS) equation and can be reduced to that form under the implications of specific conditions. Concisely, it incorporates fiber losses through the attenuation coefficient α, chromatic dispersion through β_1 and β_2, and fiber nonlinearity through γ.

4.2.1 Higher Order Nonlinear Effects

In the assumptions made towards the derivation of the propagation equation of optical pulses in a nonlinear dispersive medium such as fibers, the relative outcomes of Stimulated Raman Scattering and Stimulated Brillouin Scattering were not taken into account. Hence, the propagation Equation (4.11) in the above section may need to be modified for the same.

As brought out in earlier chapters that if optical power of the pulse which is being pumped into the fiber exceeds the threshold power level, Stimulated Raman Scattering and Stimulated Brillouin Scattering can result in the transfer of energy to an optical pulse at a dissimilar wavelength, which may traverse in the same or the reverse direction. Also, owing to the cross phase modulation (XPM) effect, the two pulses may interact with each other. But, the most significant constraint can be

imposed by disregarding of the Raman Effect i.e. the interactions of photons with phonons (molecular vibrations) of the medium.

In case of pulses having a broad spectrum, the Raman-gain can result in the amplification of the low-frequency components of a pulse by means of energy transfer from the high-frequency components of the pulse. This effect is termed as intra pulse Raman scattering. Consequently, the pulse spectrum moves towards the low-frequency region with propagation of the pulse within the fiber, an effect termed as the Raman-induced frequency shift.

Taking into account all the aforestated add-ons, we get the generalized pulse propagation equation which is as follows [4]:

$$\frac{\partial A}{\partial z} + \frac{1}{2}\left(\alpha(\omega_0) + i\alpha_1 \frac{\partial}{\partial t}\right) A - i\left(\sum_{n=1}^{\infty} \beta_n \frac{i^n}{n!} \frac{\partial^n A}{\partial t^n}\right) = i\left(\gamma(\omega_0) + i\gamma_1 \frac{\partial}{\partial t}\right) \times \left((A(z,t)) \int_0^{\infty} R(t') |A(z, t-t')|^2 dt'\right) \tag{4.14}$$

In Eq. (4.14), the terms on LHS signify the linear effect. The terms on RHS indicate the nonlinear effects. The integral part in the above mentioned equation signifies the exchange of energy arising due to intrapulse Raman scattering. $R(t')$, known as the nonlinear response function, takes into account the contributions owing to the electronic as well as nuclear effects. It is expressed as [4]:

$$R(t') = (1 - f_R)\delta(t' - t_e) + f_R h_R(t') \tag{4.15}$$

Where f_R denotes the partial contribution of the delayed Raman response to nonlinear polarization P_{NL}. The $h_R(t')$ is the Raman response function and contains information on the vibration of the molecules of the matter as light passes through it. It is given by [4]:

$$h_R(t') = \frac{\tau_1^2 + \tau_2^2}{\tau_1 \tau_2^2} \exp\left[\frac{-t'}{\tau_2'}\right] \sin\left(\frac{t'}{\tau_1}\right) \tag{4.16}$$

where τ_1 is the Raman period and τ_2 is the damping time of vibrations.

4.3 HIGHLY NONLINEAR FIBERS

Self-phase modulation (SPM), cross phase modulation (XPM) and four wave mixing constitute the three fundamental nonlinear phenomena occurring inside optical fibers.

The above mentioned effects are described in terms of a particular nonlinear parameter γ which can be redefined as [4]:

$$\gamma = \frac{2\pi n_2}{\lambda A_{eff}} \tag{4.17}$$

where,

λ : Wavelength of light;

n_2: Nonlinear Kerr coefficient, a material parameter which is fixed for each glass material and,

A_{eff}: Effective mode area given in Equation (4.13) which depends on the design of the fiber and can be reduced with proper designing techniques to increase γ.

Thus, the only way to increase γ for silica based optical fibers is to reduce the effective mode area A_{eff}. Hence, in order to design highly nonlinear fibers, non-silica glasses seem to be a viable option.

4.3.1 Tapered Fibers with Air Cladding

In 1970, a technique was introduced for tapering the optical fibers to produce fibers having a narrow core encapsulated in an air cladding in order to improvise the self-phase modulation effect. The process involved reduction in the diameter of silica cladding of a standard optical fiber from 125 μm to 2 μm and was employed for fabricating optical couplers by heating and elongating the fiber.

The process involves heating the fiber with a CO_2 laser. The heat generated by the laser mellows down the fiber. Reasonable loads joined to the two fiber finishes give the power that pulls the fiber and lessens its diameter. Amid the extending procedure, the fiber diameter is persistently watched and the laser is switched off when the ideal diameter measurement has been achieved. The final

product is a fiber with a cladding diameter reduced from 125 μm to around 2 μm. Consequently, the original fiber's cladding behaves like a core which confines the light pulse while the surrounding air acts like a cladding. Figure 4.1 shows photographs of (a) the fiber before tapering, (b) the transition region, and (c) the central region with a narrow core [4].

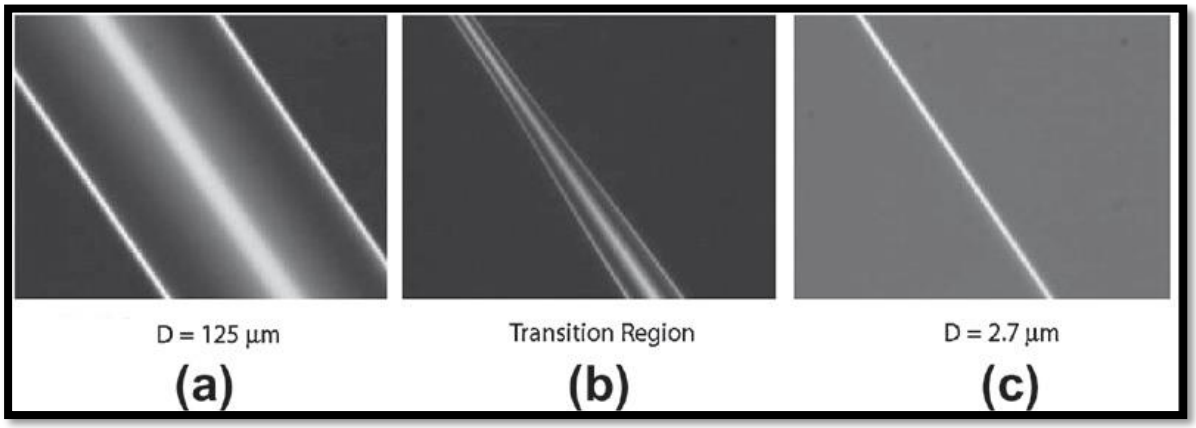

Figure 4.1: Microphotographs of (a) the original single-mode fiber, (b) the transition region, and (c) the central region with a narrow core [4].

Compared with standard fibers, a tapered fiber having 2 μm diameter has considerably high value of γ, approximately 50 times, thereby, making it a highly nonlinear fiber [4]. These high values of γ arise as a consequence of the tight confinement of light resulting due to air cladding.

4.3.2 Microstructured Fibers

In the 1970s, Kaiser and Astle proposed to alter the refractive index profile of an optical fiber by introducing a microstructure and thereby, modify its guidance properties. However, it was only with the pivotal work carried out by Russell and his colleagues during 1996 [7], that fabrication of such fibers has become common in the technological world.

Microstructured fibers (MOFs) comprise of an arrangement of small air holes running throughout their entire length and characterize the wave guiding properties. The confinement and guidance of optical fields in MOFs can be attained either by the PBG effect or modified total internal reflection. Accordingly, they are categorized as Index-Guiding Fibers and Photonic Bandgap Fibers (PBGFs).

In the year 1996, PCFs were developed for the first time [4]. They comprised of a central intertwined silica core encompassed by a standard cluster of airholes running along the length of the fiber. The number, size, and direction of the air holes surrounding the core gave further degrees of freedom that could not be realized in conventional fibers, and could be custom-made to provide extraordinary light confinement and dispersion attributes.

There are two types of photonic crystal fibers – Hollow core PCFs and Solid core PCFs. Hollow core PCFs were first realized in 1999 and been attractive since then in various applications such as lossless and distortion free transmission, particle trapping and optical sensing. In these types of fibers, the intermittent variations in refractive index inside the cladding lead to the confinement of an optical mode within the hollow core. In other words, the PBG effect is solely responsible for guiding of modes as there is no TIR inside the hollow core.

In solid core PCFs, since the core of the fibers is solid, it has a higher refractive index than the cladding comprising of air-holes. In these fibers, guidance of light takes place through modified total internal reflection. Figure 4.2 shows SEM images depicting four forms of MOFs.

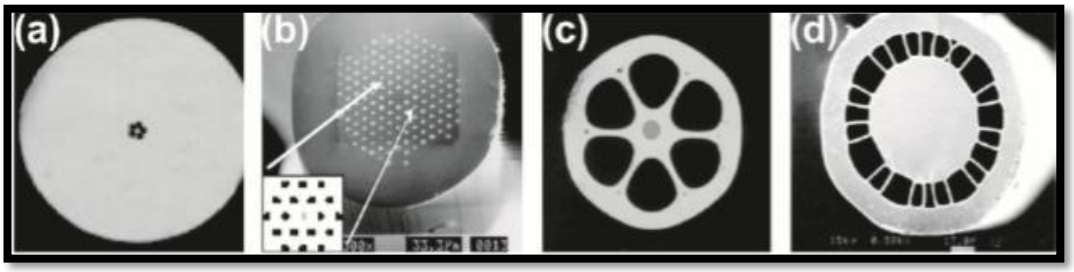

Figure 4.2: Scanning electron micrograph images depicting four forms of MOFs. (a) Narrow silica core encapsulated in a ring of air holes with a silica cladding leading to a high refractive step index.(b) PCF: Narrow silica core encapsulated invarious rings of periodic air holes (c) Grapefruit structure: Narrow silica core encapsulated inlarge air holes. (d) Core encapsulated in ring of air; narrow silica bridges linking the core and the cladding [4].

4.3.3 Chalcogenide Fibers

Although silica fiber has been successfully utilized in the demonstration of ultra-broadband light generation spanning more than an octave, the low nonlinear refractive index offered by silica still limits its practicality. Hence, several other materials including chalcogenides, silicates, tellurite and bismuth oxide have been used to make optical fibers. The value of n_2 for silica is 2.7 ×

$10^{-20}m^2/W$ at a wavelength of 1.06 μm which is much smaller than highly nonlinear glasses mentioned above [26]. Among these materials, chalcogenide glasses several advantageous features.

Chalcogenide glasses comprise of one or more elements constituting group 16 of the periodic table such as Sulphur (S), selenium (Se), and tellurium (Te), except oxygen (O_2) which are covalently attached to elements including arsenic (As), antimony (Sb), germanium (Ge),and silicon (Si), etc. [5]. These glasses are remarkable for nonlinear optics since they exhibit very high nonlinear coefficients with moderate or low absorption. These glasses have a nonlinear refractive index at least 1000 times higher than that of the silica glasses and an excellent IR and mid-IR transmission window up to 20 μm [26]. In addition, owing to the high refractive index (2.4 – 2.8), these glasses are capable of strongly confining the optical pulses. All these factors make them quite attractive for the fabrication of HNLFs.

Chapter 5

SUPERCONTINUUM GENERATION: HISTORICAL PERSPECTIVES

Since the early 1960s, great impetus has been laid in the field of nonlinear optics on the study of its characteristic features, primarily - spectral broadening and the generation of new frequency components. Specifically, the phenomenon termed as Supercontinuum Generation (SCG) occurs when ultra – short pulses of laser light, while passing through a highly nonlinear medium, undergo extreme nonlinear spectral broadening and evolve into light with a broadband spectrum [4]. In the year 1970, Alfano and Shapiro reported, for the first time, the generation of supercontinuum spectra in bulk glass [11]. The broadening of the spectra is mainly due to the interaction of linear and nonlinear effects involving dispersion, self-phase modulation (SPM), four-wave mixing (FWM), cross-phase modulation (XPM), stimulated raman scattering (SRS), and soliton associated dynamics at pump wavelength [5]. Owing to its multiple applications in various streams such as frequency metrology, optical coherence tomography (OCT), molecular spectroscopy, gas sensing, and early cancer detection, SCG has emerged as the subject of multifarious studies, investigations and analysis on a diverse range of nonlinear media comprising of different types of waveguides.

Although SCG was first reported in 1976 in optical fibers, the advent of microstructured optical fibers, among which the PCFs form a subset, made the utilization of optical fibers quite universal for the generation of supercontinuum spectra. The various features of PCFs which make them the most suitable candidate for generating supercontinuum are their enhanced modal confinement, thereby, resulting in improved nonlinearity and the capability to tailor their dispersion attributes by varying the requisite geometrical parameters. The exemplary freedom displayed by the PCFs in terms of modifying its design parameters allowed the generation of supercontinuum over a considerable array of pumping source parameters which was earlier not feasible with conventional optical fibers.

5.1 OVERVIEW OF RESULTS

5.1.1 Experimental Outcomes in Bulk media

The absolute first perception of supercontinuum generation (SCG) was made by Alfano and Shapiro (1970) in which they demonstrated the formation of white light spectrum crossing over the whole range from 400 to700 nm. The spectrum was realized by transmitting 5 mJ picosecond pulses at530 nm in BK7 glass [11]. Subsequently, analogous results were stated in another experiment carried out by Bondarenko *et al.* (1970). Although broadening of the laser light spectrum in a nonlinear fashion had been accounted for earlier by Stoicheffin in 1963 and by Brewer in CS_2 in 1967, it was the comprehensive spread of the spectrum of the produced light, almost multiple times more extensive than anything recently announced, which gave gigantic imperativeness to the experiment carried out by Alfano and Shapiro. Since the work carried out by Alfano and Shapiro was exclusively committed to the underlying acknowledgment of the phenomenon of “four - wave mixing", the expression "supercontinuum" was nowhere used in their paper. During those days, the supercontinuum effect was stated as either superbroadening effect (Bondarenko *et al.,* 1970; Il'ichev *et al.*, 1972), anomalous frequency broadening (Werncke *et al*., 1972; Bloembergen, 1973), or white-light continuum (Fork *et al*., 1983) [2].

Initially, the major cause responsible for supercontinuum generation in bulk media was attributed to the self-focussing effect. Self-focussing is a nonlinear optical process that takes place as a result of the optical Kerr effect. When a light beam of high intensity propagates through a highly nonlinear medium, then the refractive index of the medium increases with the electric field intensity and it starts to act as a lens leading to the focusing of the beam as it travels through the medium. This leads to a decrease in the beam radius and as the optical intensities become even higher, it may lead to a total collapse of the beam. Also, the very high optical intensities can result in completely destroying the optical medium, when the optical power reaches above the critical power.

It was the work by Gaeta [2], using 3-D simulations of light propagation, that established the fact that self-focussing was primarily responsible for supercontinuum generation in bulk media and thus, confirmed analyses of the earlier experiments in this regard. In view of the above mentioned facts, it can be opined that SC generation in bulk material is significantly an intricate phenomenon involving complex amalgamation between diverse effects in space and time [2].

5.1.2 Experimental Outcomes in Conventional Fiber

Initial experimentations on supercontinuum generation in optical fiber were executed by pumping high intensity pulses constituting the visible spectrum of light into a silica-based optical fiber with zero dispersion wavelength at around 1.3 μm. In 1976, experiments were carried out by Lin and Stolen who utilized highly intense pulses in the scope of couple of kilowatts, delivered from a laser so as to produce a supercontinuum in the range of 200 THz [2]. Subsequently, visible region pump pulses (10 ps–10 ns) were utilized to carry out generation of supercontinuum which delivered comparable results [2]. The resulting spectral broadening was accredited to the interplay between the various nonlinear phenomena such as SPM and XPM, Raman scattering, four wave mixing, etc.

Now, when the pumping of pulses is carried out in the normal dispersion regime, the broadening of the spectrum occurs as a result of mutual interaction between Raman scattering and SPM. On the other hand, when pumping is executed in the anomalous dispersion regime, it is the consequence of generation of optical soliton and their associated dynamics that leads to spectral broadening. This aspect was first brought out by Hasegawa and Tappert (1973) [2], as a result of the analysis of the nonlinear Schrödinger equation (NLSE).

It was Golovchenko whose work elucidated and explained the involvement of soliton dynamics and Raman scattering in supercontinuum generation, using ultrafast pump pulses, in the anomalous dispersion regime during 1990-91.

5.1.3 Experimental Outcomes in Photonic Crystal Fiber

Although in 1970s, it was suggested that the guidance characteristics of the optical fibers could be altered by incorporating a microstructure in their refractive index profile (Kaiser and Astle, 1974), it was the pivotal work of Russell and his colleagues that made the fabrication of such fibers technologically possible in 1996. Since these fibers had the peculiar characteristic of confining and guiding light through the phenomenon of photonic band-gap effect, these fibers were termed as photonic crystal fibers (PCFs).

In 2000, Ranka *et al.* demonstrated the generation of a supercontinuum spectra ranging from 400 to 1500 nm in only 75 cm of photonic crystal fiber using 100 fs pulses from a Ti:sapphire laser [2]. Later on, by using similar pump pulse parameters and PCF, Wadsworth *et al.* [2], reported the generation of supercontinuum spectra from the UV to IR realm of wavelengths, in spite of the fact that the exact degree of broadening was not explicitly expressed. These outcomes were recognized as very striking since past work executed in this direction had required progressively complex sources with pulse energies at the micro joule level. It was sooner understood that SCG will emerge as a extensively available technology with the simultaneous advent of dispersion-engineered PCFs and femtosecond Ti:sapphire lasers. However, even at this point, there was still no reckonable explanation that could elucidate the physics underlying the widening of the light spectrum, despite the fact that the SC spectra generated using photonic crystal fibers were being utilized in various applications.

It was only in the year 2000 that Birks *et al*. carried out an experiment that successfully explicated the fact that it was the interplay among the dispersion and diverse nonlinear phenomena that plays a key role in the supercontinuum generation process in PCF. Owing to the extensive studies, experiments and analyses, the elementary mechanisms and phenomena leading to supercontinuum generation in photonic crystal fibers were undoubtedly ascertained by 2002. It was deciphered that the creation of long-wavelength components of the supercontinuum spectra was attributable to soliton fission along with Raman self- frequency shift and the short-wavelength components were generated due to the dispersive wave dynamics.

5.2 EXPERIMENTAL DESIGN GUIDELINES FOR SC GENERATION

SCG is an intricate process and any reckonable clarification of the allied phenomena must consider various parameters associated with the fiber and the pulse. Nevertheless, considering from the application point of view, it is often more crucial to have the know-how of selecting an efficient pumping source and the type of fiber so as to produce a supercontinuum with specific desirable attributes than physics underlying supercontinuum generation process.

Let us have an understanding of some relatively straightforward practical guidelines based on various investigations and analyses that can go a long way is assisting the various facets of experimental design for SC generation.

Applications involving biomedical imaging, optical coherence tomography, molecular spectroscopy, etc. necessitate the generation of a phase-stable continuum which implies the requirement of a femtosecond pulse source. Since, ideally, one prefers to use minimum fiber length, a vital guideline in this aspect will be to utilize pumping pulses with optimum power in order to attain the requisite bandwidth using minimal length of the fiber. Owing to experimental uncertainties, it is advisable to initiate the work with a longer length and subsequently reduce the length in order to optimize the SC characteristics [2].

If pumping is carried out in the normal dispersion region, then supercontinuum produced will not encompass any fine structure desirable in the context of communications. Although selecting a pump source in the normal dispersion region will lead to superior coherence properties, but the same will be achieved at the expense of an abridged bandwidth.

Further, in applications wherein the coherence properties are inconsequential, the efficacy of the source of supercontinuum depends on its effective brightness and wide bandwidth. Hence, for such applications, a high power source along with an apposite PCF can be employed for SCG. By choosing a pump wavelength close to the ZDW, one can expect optimum bandwidth and spectral flatness [2].

Chapter 6

SUPERCONTINUUM GENERATION USING $Ge_{11.5}As_{24}Se_{64.5}$ BASED MICROSTRUCTURED OPTICAL FIBER

This chapter deals with the generation of a supercontinuum spectrum in the mid-infrared region using $Ge_{11.5}As_{24}Se_{64.5}$ based microstructured optical fiber. Although the visible and near-infrared regions are covered by commercial supercontinuum sources, the mid-infrared range of wavelengths is still under extensive research. SCG in the mid-infrared realm is crucial because mid-infrared spectroscopy can go a long way in elucidating the molecular structures of the matter and performing nonintrusive diagnostics of chemical, physical, and biological systems of interest [12]. In this work, a finite element method based software "COMSOL Multiphysics" has been employed to execute the geometrical design of the microstructured optical fiber in $Ge_{11.5}As_{24}Se_{64.5}$ chalcogenide glass and to calculate the effective refractive index (n_{eff}) and effective area of the Fundamental mode (A_{eff}) for different wavelengths along with variation of the controlling parameters of the MOF. Subsequently, the group velocity dispersion (GVD) along with other higher-order dispersion parameters are also calculated. Further, the nonlinear refractive index of the material n_2, effective mode area A_{eff} and the nonlinear coefficient γ are also calculated. In order to achieve a broadened spectrum, the geometrical parameters of the fiber such as diameter of the air holes and their respective center-to-center distance have been manipulated in order to obtain minimum dispersion and minimum A_{eff} at the pump wavelength which is chosen close to the ZDWL. During the simulation, the effect of various parameters like peak power, pulse width and length of the fiber are considered to study the nature of SC and the best broadening has been demonstrated at a -30 dB power level.

6.1 MID INFRARED REGION AND $Ge_{11.5}As_{24}Se_{64.5}$ CHALCOGENIDE GLASS

Although dispersion engineering due to the strong modal confinement can be achieved in silica photonic crystal fibers, however, in order to achieve a broad supercontinuum generation spectra, the requirement of a pumping source with a very high peak power is essential owing to the weak nonlinearity of the silica. Also, since silica exhibits significant absorption beyond 2.4 μm, it puts limitation on the generation of a broader supercontinuum spectrum in the mid-infrared domain. Hence, it is impossible to extend the broadening of the supercontinuum spectra in the mid-infrared domain beyond 2.4 μm using the fiber or waveguide geometries in the silica material.

The mid-infrared region extends from about 2 μm to 20 μm. It has two windows (3-5 μm and 8-13 μm) wherein the Earth's atmosphere is comparatively translucent [8,10]. Further, the mid-infrared molecular fingerprint region ranging from 2-15 μm can be used for various applications in the fields of astronomy and security [8,10]. In the medical field, it can be used for cancer diagnostics as the mid-infra domain can be used to make a tissue spectral map which provides information about the existence of malevolent tissues [12].

Materials like tellurite, bismuth, fluoride, and chalcogenides demonstrate considerable optical nonlinearities and optical transparency in the near to MIR range of wavelengths, thereby, making them quite apposite for supercontinuum generation in the said realm of wavelengths. Amid all the nonlinear glasses, chalcogenide glasses have emerged asexceptional contenders for supercontinuum generation in the MIR region owing to their optical transparency up to 25 μm in the infrared realm of wavelengths. Further, chalcogenide glasses exhibit extraordinarily high nonlinearity amid all glasses which makes them exceptionally good materials for the fabrication of planar waveguides for supercontinuum generation in the mid infrared region.

Chalcogenide materials such as As_2S_3, As_2Se_3, $Ge_{11.5}As_{24}S_{64.5}$ and $Ge_{11.5}As_{24}Se_{64.5}$ glasses are extremely apposite for fabricating active and passive devices in the mid-infrared expanse of wavelengths. Among the aforestated glasses, $Ge_{11.5}As_{24}Se_{64.5}$ glass has got exceptional film-forming characteristics along with

appreciable thermal and optical stability even when subjected to light with high intensity [25].

In this analysis therefore, $Ge_{11.5}As_{24}Se_{64.5}$ glass is used to design the fiber for SCG in the mid-infrared region.

6.2 PROPOSED Ch-MOF DESIGN

The cross-sectional interpretation of the proposed $Ge_{11.5}As_{24}Se_{64.5}$ based microstructured optical fiber is shown in figure 6.1. As illustrated in the figure, air-holes are arranged symmetrically in a rectangular lattice pattern, having diameter '*d*' and the center-to-center distance of air-holes is denoted by '*Λ*'. One air-hole has been removed for the confinement of the propagating fundamental mode in the proposed design. This MOF is surrounded by a perfectly matched layer (PML) of width 1μm which is used at the boundaries to avoid reflections and to optimize the results obtained. From the fabrication point of view, the reported Ch-MOF structure can be fabricated using the commonly employed technique of "stack and draw". The electric field distribution of the fundamental mode propagating in the fiber simulated at a pump wavelength of 3.1 μm is shown in figure 6.2.

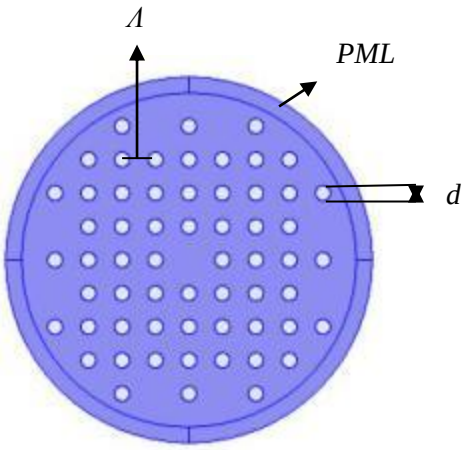

Figure 6.1: Transverse cross section of the proposed Ch-MOF.

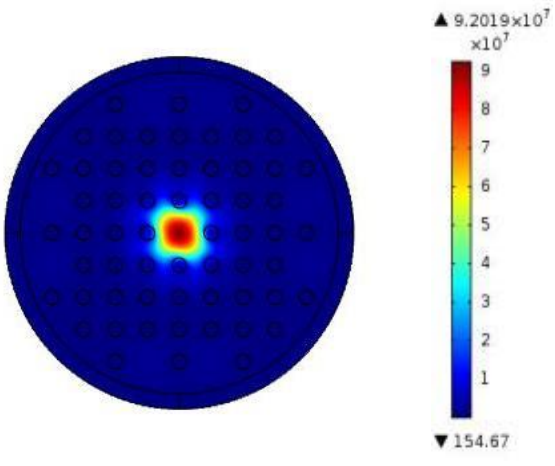

Figure 6.2: Simulated electric field distribution of the fundamental mode at the pump wavelength of 3.1 μm.

6.3 METHOD OF ANALYSIS

The SCG is governed by the following nonlinear Schrodinger equation (NLSE) [4]:

$$\frac{\partial A}{\partial z} + \frac{\alpha}{2}A - \left(\sum_{n\geq 2}\beta_n \frac{i^{n+1}}{n!}\frac{\partial^n A}{\partial t^n}\right) = i\gamma\left(1 + \frac{i}{\omega_0}\frac{\partial}{\partial t}\right) \times \left((A(z,t)) \int_{-\infty}^{\infty} R(t')|A(z,t-t')|^2 dt'\right) \tag{6.1}$$

In Eq. (6.1), the terms on LHS connote the linear effect while the terms on RHS indicate the nonlinear effects. The output pulse envelope is denoted by $A(z,t)$. The symbol 'n' is related to order of the dispersion effect. The term β_n is called the dispersion parameter of n^{th} order and term γ is called the nonlinear coefficient. These terms can be optimized by tailoring the geometrical parameters of the fiber. Also, the nonlinear coefficient will have optimal value, if the effective mode area of the fundamental mode is minimal. The aim of the design is to satisfy the above two conditions in order to achieve a broader supercontinuum spectrum.

6.3.1 Linear Characteristics

The wavelength dependent refractive index is calculated using Sellmeier's equation [5]:

$$n(\lambda) = \sqrt{1 + \frac{A_1\lambda^2}{\lambda^2 - B_1^2} + \frac{A_2\lambda^2}{\lambda^2 - B_2^2}} \tag{6.2}$$

where A_1 = 5.78525, A_2 = 0.39705, B_1 = 0.28795, B_2 = 30.39338, and λ is the pump wavelength in micrometers [5]. Equation (6.2) is employed to calculate the effective mode index of the fundamental mode using COMSOL Multiphysics software. The software can be used for modelling various engineering applications including heat transfer, fluid flow and electromagnetics.

For the generation of SCG, since the input waveforms are short optical pulses, GVD is also taken into account. The dispersion D is calculated using the relation [4]:

$$D(\lambda) = \frac{-\lambda}{c}\frac{d^2 \mathrm{Re}\,(n_{eff})}{d\lambda^2} \tag{6.3}$$

where Re(neff) is the real part of effective refractive index and c is the velocity of light in free space.

As the refractive index is frequency dependent, pulses with considerable spectral width will be subjected to chromatic dispersion. This may be considered by expanding the mode-propagation constant β in a Taylor series about the pulse's central frequency ω. This can be mathematically represented as [1,4]:

$$\beta(\omega) = \beta_0 + \beta_1(\omega - \omega_0) + \frac{1}{2!}\beta_2(\omega - \omega_0)^2 + \cdots \tag{6.4}$$

where

$$\beta_m(\omega) = \left(\frac{d^m \beta}{d\omega^m}\right)_{\omega = \omega_0} \qquad (m = 0,1,2 \ldots)$$

The first term on the RHS of equation (6.4) represents the effective refractive index of the propagating mode while the second term signifies the group velocity, and the third term denotes the group velocity dispersion (GVD) of the pulse.

6.3.2 Nonlinear Characteristics

As brought out in section (6.3), the RHS of equation (6.1) comprises of nonlinear terms and nonlinear effects like nonlinear coefficient γ, SPM, XPM, FWM, and SRS. This nonlinear coefficient γ relies on the material's nonlinear Kerr coefficient and is given by [4]:

$$\gamma = \frac{2\pi n_2}{\lambda\, A_{eff}(\lambda)} \mathrm{m}^{-1}\mathrm{W}^{-1} \tag{6.5}$$

where n_2 denotes the nonlinear refractive index of the material. The value of n_2 for $Ge_{11.5}As_{24}Se_{64.5}$ chalcogenide glass material is 4.3 $\times 10^{-18}$ m^2/W at 3.1 μm and α = 0.6 dB/cm [5]. Aeff, called the effective mode area, is a function of the wavelength and is given by [4]:

$$A_{eff} = \frac{\left(\iint_{-\infty}^{\infty} |E(x,y)|^2 \, dxdy\right)^2}{\iint_{-\infty}^{\infty} |E(x,y)|^4 \, dxdy} \tag{6.6}$$

where E(x,y) is the transverse electric field of the fundamental mode.

$R(t')$, known as the nonlinear response function, takes into account both the electronic as well as nuclear effects. It is expressed as [4]:

$$R(t') = (1 - f_R)\delta(t' - t_e) + f_R h_R(t') \tag{6.7}$$

where f_R denotes the partial contribution of the delayed Raman response to nonlinear polarization P_{NL}. For $Ge_{11.5}As_{24}Se_{64.5}$ chalcogenide glass, f_R is 0.031 [5]. The $h_R(t')$ is defined as the Raman response function and includes information pertaining to the vibration of the molecules of the matter as light passes through it. It is given by [4]:

$$h_R(t') = \frac{\tau_1^2 + \tau_2^2}{\tau_1 \tau_2^2} \exp\left[\frac{-t'}{\tau_2'}\right] \sin\left(\frac{t'}{\tau_1}\right) \tag{6.8}$$

where $\tau_1$is the Raman period and τ_2 is the damping time of vibrations. For $Ge_{11.5}As_{24}Se_{64.5}$ chalcogenide glass, τ_1= 15.5 fs and τ_2= 230.5 fs [5].

Now, in order to achieve a broader supercontinuum spectra, the nonlinear parameter should be as high as possible. As brought out by equation (6.5), this can be realized by either increasing n_2 (by the selection of appropriate material) or by decreasing A_{eff}. Since the effective mode area is design dependent, it can be optimized by varying the diameter of the air holes in a high nonlinear refractive index fiber [10].

Therefore, the overall endeavor in the design of the microstructured fiber is to optimize both the dispersion curve and nonlinearity such that at the pump wavelength both dispersion and A_{eff} are minimized so as to achieve a broad SCG.

6.4 RESULTS AND DISCUSSION

Dispersion management property is basically controlled by the geometrical parameters (pitch and size of air-holes) of the proposed Ch-MOF design. A thorough analysis has been carried out by varying the diameter of the airholes and their center-to-center distance and the design has been optimised to obtain minimum dispersion at a pump wavelength of 3.1 μm with a minimum effective

mode area. Initially, the effect of variation in the diameter air-holes has been studied, keeping the other parameter fixed i.e. the center-to-center distance between the airholes at Λ=2.1 μm, and is shown in figure (6.3).The diameter of the air-holes is varied from 0.92 μm to 0.96 μm to obtain low dispersion at the pump wavelength. With an increase of '*d'* parameter, the effective mode area decreases and the zero dispersion wavelength shifts towards the shorter wavelength side. The dispersion at the pump wavelength of 3.1 μm is varied from 2.36 ps/nm-km at d = 0.96 μm to -2.7 ps/nm-km at d = 0.92 μm. The effective mode area varied from 8.94 μm^2 to 8.5 μm^2 as '*d'* was varied from 0.92 to 0.96 μm.

Figure (6.4) demonstrates the variation in the dispersion characteristics by changing the pitch (Λ) i.e. the center-to-center distance between the airholes. On increasing the parameter Λ, ZDWL shifts towards the longer wavelength side. The dispersion value changes from 15.1 ps/nm-km to -11.52ps/nm-km as Λ is increased from 1.9 to 2.3 μm at the pump wavelength of 3.1 μm. The effective mode area changes from 6.6 to 11.1 μm^2 for the above variation. From the above discussion, it can be noted that for the structural parameters d=0.94 μm and Λ=2.1μm, dispersion of -0.12 ps/nm km has been obtained with an effective mode area 8.71 μm^2, at a pump wavelength of 3.1 μm.

The optimized dispersion characteristic curve between 1-12 μm for geometrical parameters d=0.94 μm and Λ=2.1 μm is demonstrated in figure (6.5). The structure has high dispersion until 2.5 μm in a normal dispersion region. It has minimum dispersion at pump wavelength i.e. 3.1 μm, anomalous dispersion between 3.15–4.3 μm, and normal dispersion between 4.35–12 μm. From the dispersion characteristics, it is evident that the structure has a flat dispersion over a wide range. This helps for an efficient continuum generation.

The variation of nonlinear coefficient γ and effective mode area for optimized parameters at different wavelengths are shown in figure (6.6). The effective mode area (blue solid line) increases with an increase in wavelength. On the contrary, the nonlinear coefficient (green solid line) decreases with an increase in wavelength. At a pump wavelength of 3.1 μm the proposed structure exhibits a nonlinear coefficient of the order of 1001 W^{-1}/km and an effective mode area of 8.71 μm^2 for optimized parameters d=0.94 μm and Λ=2.1 μm.

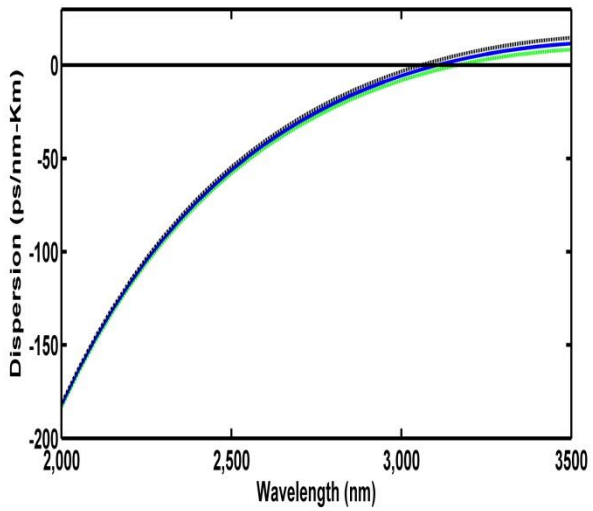

Figure 6.3: Influence on the dispersion characteristics with the variation of diameter of the air holes, d.

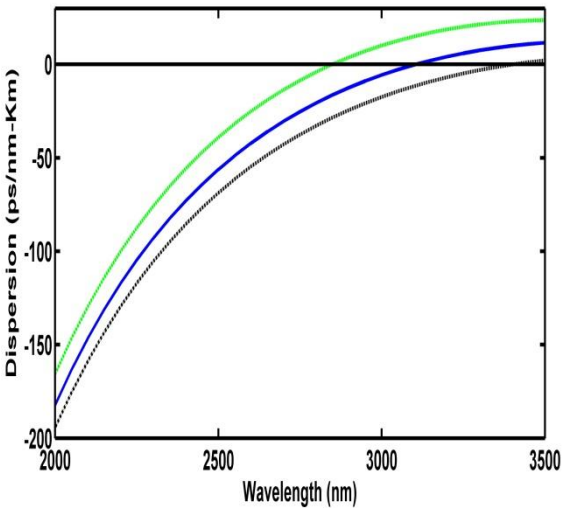

Figure 6.4: Influence on the dispersion characteristics with the variation of center-to-center distance of airholes, Λ.

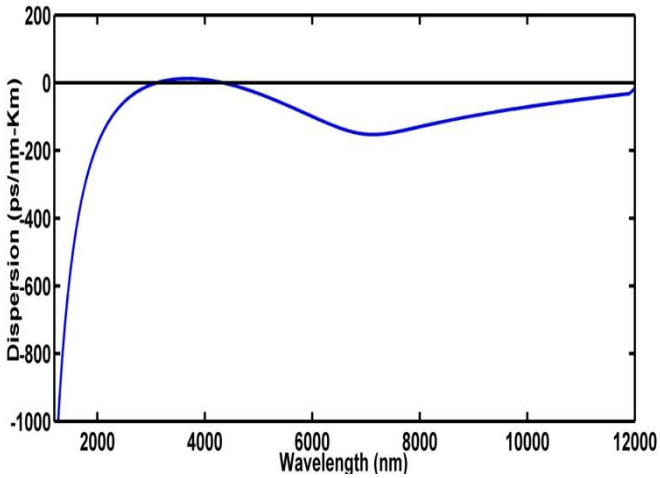

Figure 6.5: Dispersion characteristics of the proposed design.

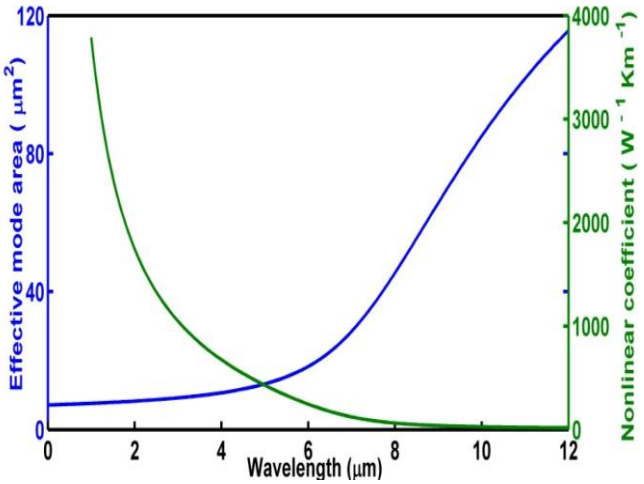

Figure 6.6: Variation of the nonlinear coefficient and effective mode area against wavelength.

6.5 SUPERCONTINUUM GENERATION

The SCG has been generated by solving equation (6.1) using MATLAB. The LHS of Eq. (1) has a dispersion parameter β_n, where 'n' is the order of dispersion. In our simulation, the order of dispersion coefficient has been considered till 9^{th} order since it was observed that increasing the dispersion till 9^{th} order had a considerable impact on the generated supercontinuum spectrum. As the limit of the order of dispersion was enhanced beyond 9^{th} order, less significant variation was noticed in the output spectrum of SC. Consequently, the 9^{th} order of dispersion was chosen. The broadening of the input pulse takes place as a result of interplay among nonlinear processes like self-phase modulation (SPM), cross phase modulation (XPM) and Raman effect. Basically, two nonlinear factors SPM and XPM are responsible for the initial broadening of input pulse when a short high intensity pulse is made incident on a nonlinear fiber in a very small effective mode area. Subsequently, as the pulse propagates inside the fiber, the high intensity electric fields interact with each other and with dielectric media, which leads to spectral broadening owing to SPM in the initial phase, followed by XPM, FWM and SRS. During the simulation, the effect of various parameters like pulse power, pulse width, and fiber length has been analyzed since these are the vital parameters which greatly influence the broadening of supercontinuum. The respective results are depicted in figures 6.7-6.9.

As depicted in figure 6.9, when optical pulses having pulse width of 50fs and peak power of 4 kW are launched in 20mm length of the proposed fiber, a broadband spectrum spanning 1.4-16 μm at a -30 dB level was obtained.

In figure 6.7, the influence of pulse width of a secant hyperbolic pulse on the SC spectrum generated in a 20 mm length of proposed fiber is depicted. The input peak power is fixed at 4000 W. To study the influence, pulse width is varied from 50 fs to 200 fs in steps of 50fs. As depicted in figure 6.8, the spectral broadening decreases as the pulse width increases from 50fs to 200fs. This is due to the fact that, when shorter pulses are utilized, it results in a broader SCG because the rate of change of intensity is high for shorter pulse widths and hence, it leads to an effective SPM, followed by other nonlinear phenomena involving XPM, SRS and FWM. However, at high pulse widths, the rate of change of intensity reduces the SPM effect, thus giving a narrower spectrum.

Figure 6.8 depicts the effect of fiber length on SCG. In order to analyze the effect of fiber length on supercontinuum generation, a secant hyperbolic pulse having pulse width of 50 fs at a peak power of 4000 W has been used for simulation and analysis. During the simulation, the fiber length was varied from 0 mm to 20 mm in steps of 5 mm. As illustrated in the figure, with increase in the length of the fiber, the SC generated broadens. Initially, the broadening occurs owing to self-phase modulation and as the pulse travels inside the fiber, other nonlinear effects such as SRS, XPM and FWM come into play resulting in further broadening.

At 20mm length of the fiber, maximum broadening occurs indicating that the entire nonlinear process is complete. Beyond 20 mm, there is no spectral broadening; instead the pulse experiences attenuation losses particularly in the shorter and longer wavelength regions [5].

The effect of variation of peak power on SC spectrum is illustrated in figure 6.9. Here, the fiber length and the input pulse duration are kept fixed at 20mm and 50fs respectively. Simulation results show that with an increase in peak pump power, the SC spectrum becomes broader. Basically, Stimulated Raman Scattering is responsible for broadening of the spectrum in the longer wavelength regions (Stokes Wave). Also, since it is intensity dependent, hence, with increase in peak power of the source, the intensity increases thereby, leading to generation of more Stokes Wave. These Stokes Waves result in broadening of the input pulse particularly in the longer wavelength regions but, until a certain peak power. After this critical value, any further increase in peak power only results in further flattening of the SC spectrum. This is because the further increase in power is balanced by the losses experienced in the extremely long and short wavelength regions [5].

Thus, it is evident from the simulations that optimum broadband SC spectra spanning over 1.4 μm to 16 μm is obtained utilizing 20 mm length of fiber pumped with 50 fs input pulses of 4 kW peak power at a pump wavelength of 3.1 μm.

Table 6.1 indicates the optimized input pulse parameters for SC generation. Table 6.2 shows a comparison of results obtained in the proposed Ch-MOF with Reference [19] and Reference [20] and indicates the upgraded results of this study.

Table 6.1: Optimized input pulse parameters.

Optimized dimensions	**Pump Wavelength**	**Dispersion**	**Nonlinear Coefficent**	**Effective Mode Area**	**SCG**
d= 0.94 µm; Λ=2.1 µm	3.1µm	-0.12 ps/nm-km	1001 $W^{-1}km^{-1}$	8.71 μm^2	1.4-16µm

Table 6.2: Comparison of results obtained in this study with Reference [19] and Reference [20].

Parameter	**Ch-MOF**	**Reference [19]**	**Reference [20]**
Core Material	$Ge_{11.5}As_{24}Se_{64.5}$	$Ge_{11.5}As_{24}Se_{64.5}$	$Ge_{11.5}As_{24}Se_{64.5}$
Nonlinearity	1001 W^{-1} km^{-1}	1431 W^{-1} km^{-1}	2317 W^{-1} km^{-1}
Fiber Length	20 mm	10 mm	100 mm
Input Power	4 kW	4 kW	3 kW
Pulse width	50 fs	50 fs	85 fs
SC- Spectrum	1.4-16µm	1.5-13 µm	1-10µm

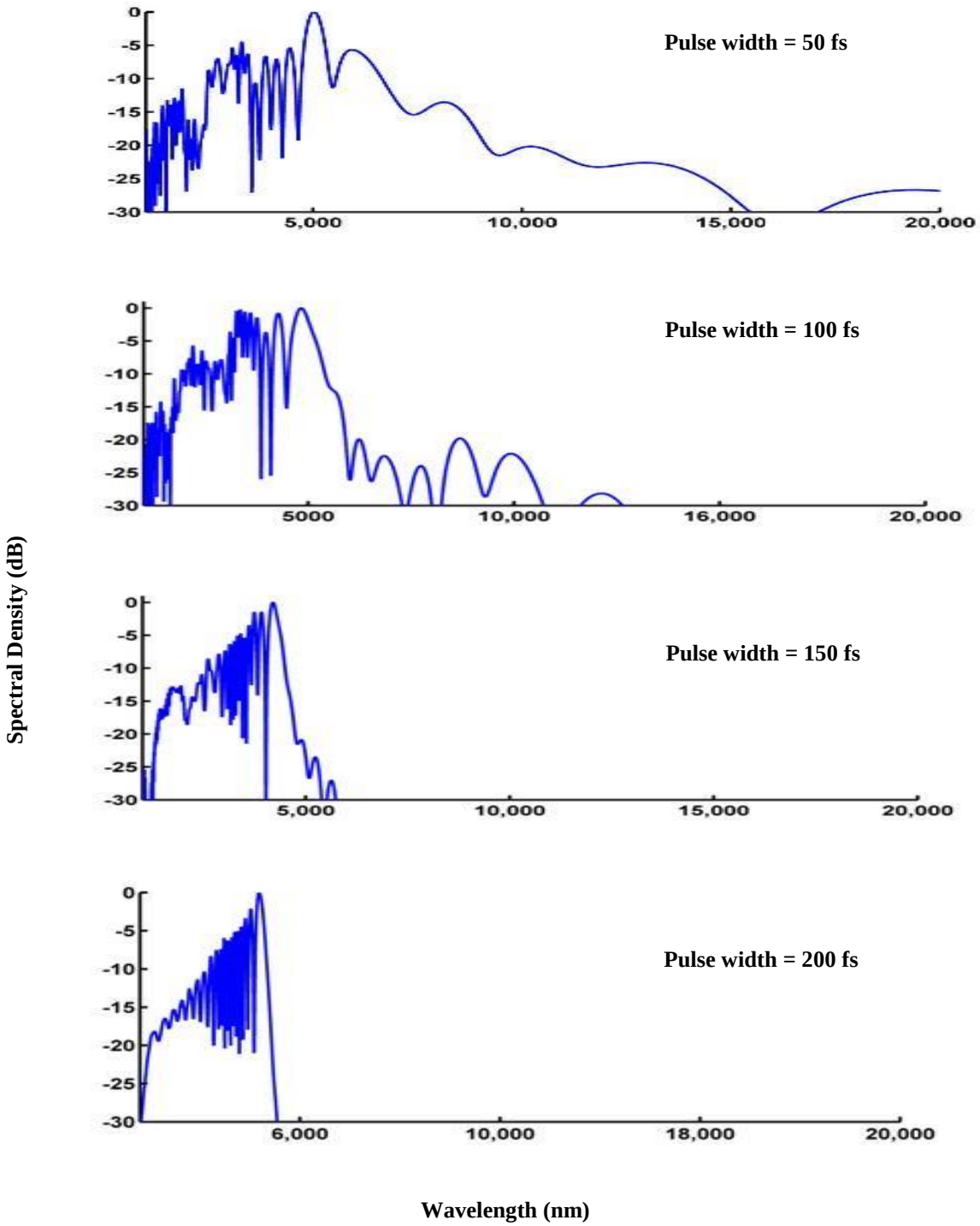

Figure 6.7: Effect of variation of input pulse width on SC spectra with a peak power of 4 kW in 20 mm length of fiber.

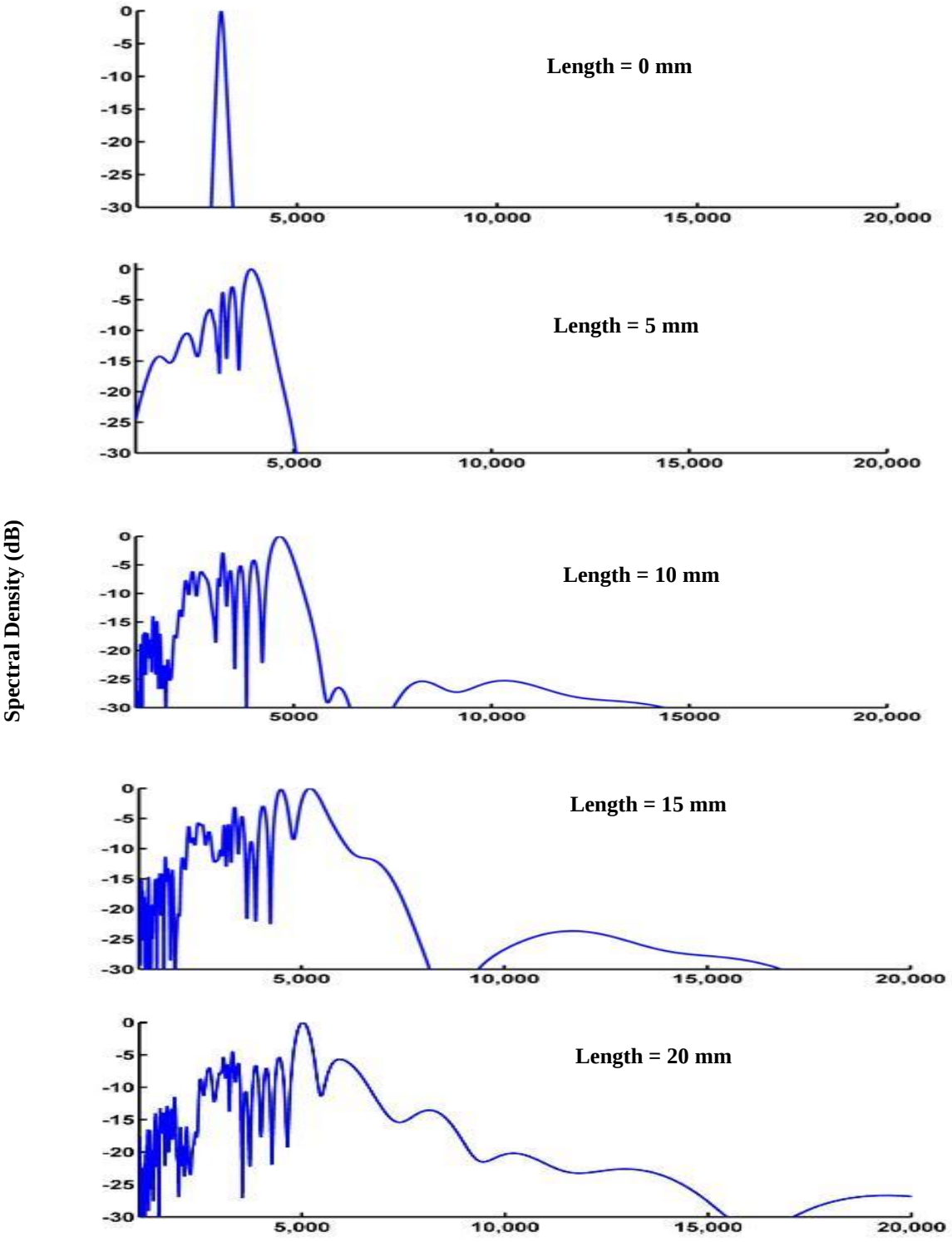

Figure 6.8: Effect of variation of length of fiber on SC spectra with 50 fs incident pulses at peak power of 4 kW.

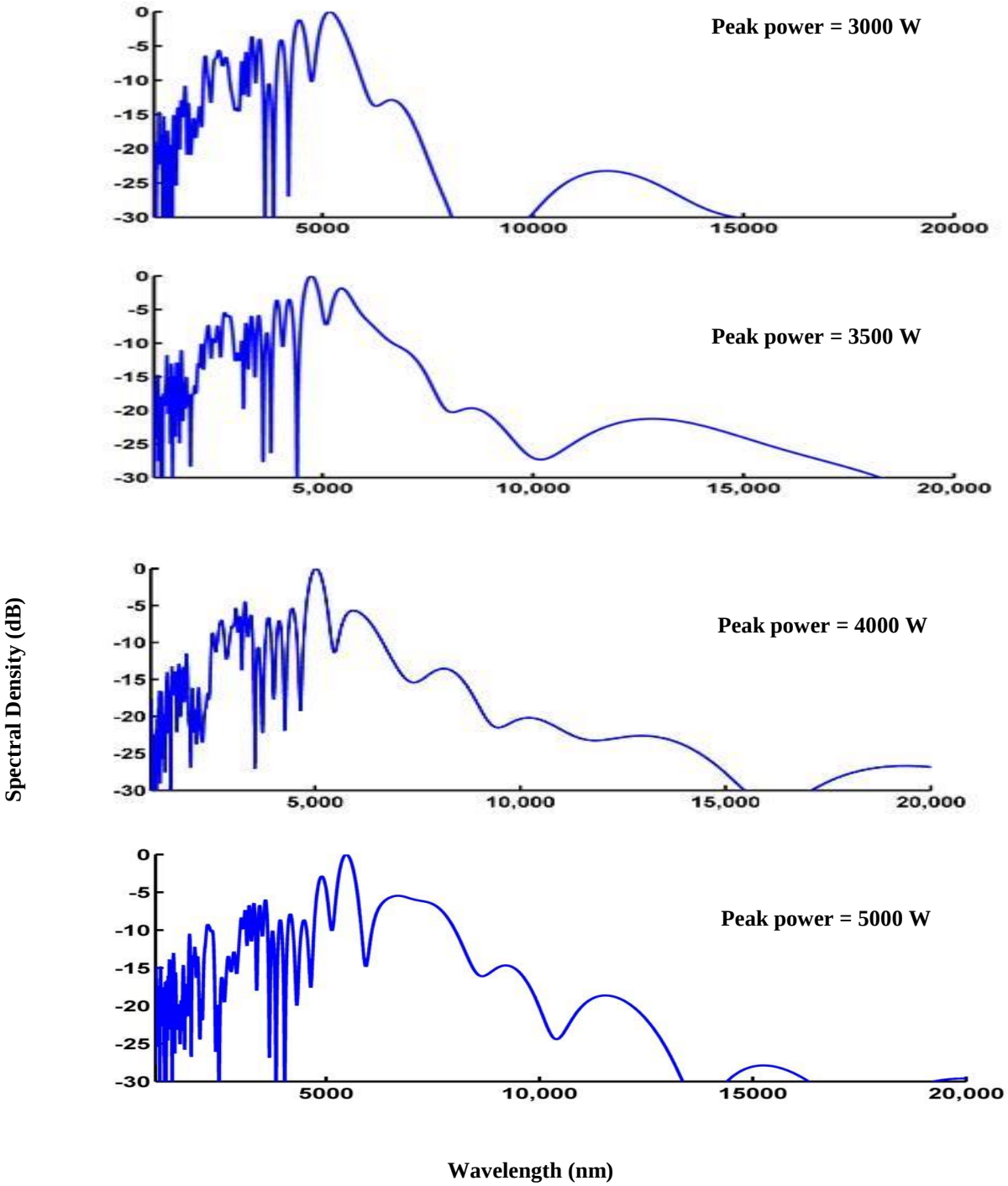

Figure 6.9: Effect of variation in peak power on SC spectra with 50 fs incident pulses in 20 mm length of fiber.

6.6 CONCLUSION

A novel $Ge_{11.5}As_{24}Se_{64.5}$ based chalcogenide glass microstructured optical fiber (Ch-MOF) structure has been designed for ultra-broadband SCG in mid-infrared regime covering 3-5 μm and 8-13 μm of spectrum region respectively and the molecular "fingerprint region" from 2-15 μm . The structure possesses a very high nonlinearity (1001 $W^{-1}Km^{-1}$) with a very low dispersion value of -0.12 ps/nm-km at a pump wavelength of 3.1 μm. A wideband supercontinuum spectrum ranging from 1.4 μm to 16 μm is generated using 20 mm of the Ch-MOF by launching 50 fs hyperbolic secant optical pulses with a peak power of 4 kW. Such broadband mid-IR SC is suitable to have significant applications in various domains including early cancer detection, spectroscopy, optical coherence tomography, frequency metrology and sensing.

6.7 FUTURE SCOPE

Since the growth of supercontinuum sources has been entwined with improvements in PCF designs, it can be very well stated that future supercontinuum sources will display high temporal coherence, enhanced bandwidth, and spectra far reaching into the infrared. Although today, MOF based supercontinuum sources are quite common and commercially available (in the visible and near-infrared regions) in all sorts of laboratories around the world however, the mid-infrared range of wavelengths is still under extensive research. Further, turnkey projects and research are required to be undertaken to bring down the cost of these sources in order to alleviate their availability and employability as they have got a wide array of applications in various fields.

References

[1] A. K. Ghatak and K. Thyagarajan, "*Introduction to fiber optics",* Cambridge University Press, 2011.

[2] J. M. Dudley, G. Genty, and S. Coen, *"Supercontinuum generation in photonic crystal fiber",* The American Physical Society, vol. 78, pp. 1135-1184, 2006.

[3] J. M. Senior, "*Optical Fiber Communication, Principles and Practice"*, 3rd ed. (Pearson Education, 2010).

[4] G. P. Agrawal, "*Nonlinear Fiber Optics"*, 5th ed. Elsevier Academic Press, 2013.

[5] A. G. N. Chaitanya, T. S. Saini, A. Kumar, and R. K. Sinha, *"Ultra broadband mid-IR supercontinuum generation in* $Ge_{11.5}As_{24}Se_{64.5}$ *based chalcogenide graded-index photonic crystal fiber: Design and Analysis",* Applied Optics, vol. 55, no. 36, p. 10138, 2016.

[6] T. S. Saini, U.K Tiwari, and R. K. Sinha, *"Rib waveguide in Ga-Sb-S chalcogenide glass for on-chip mid-IR supercontinuum sources: Design and Analysis,*" Journal of Applied Physics122, 053104 (2017).

[7] P.S.J. Russell, *"Photonic crystal fibers",* Science, vol. 299, p. 358–362, 2003.

[8] T. S. Saini, A. Kumar, and R. K. Sinha, *"Design and modelling of dispersion-engineered rib waveguide for ultra-broadband mid-infrared supercontinuum generation,*" Journal of Modern Optics, vol. 64, no. 2, pp. 143–149, Feb. 2016.

[9] M. R. Karim, B. M. A. Rahman, and G. P. Agrawal, *"Dispersion Engineered* $Ge_{11.5}As_{24}Se_{64.5}$ *nanowire for supercontinuum generation: A Parametric Study,*" Opt. Express 22, 31029–31040 (2014).

[10] T. Saini, A. Baili, A. Kumar, R. Cherif, M. Zghal, and R. Sinha, *"Design and analysis of equiangular spiral photonic crystal fiber for mid-infrared supercontinuum generation",* Journal of Modern Optics, vol. 62, no. 19, pp. 1570–1576, Sep. 2015.

[11] R. R. Alfano and S. L. Shapiro, *"Emission in the Region 4000 to 7000 Å Via Four-Photon Coupling in Glass",* Physical Review Letters, vol. 24, no. 11, pp. 584–587, 1970.

[12] T.S. Saini, A. Kumar, and R. K. Sinha, *"Broadband Mid-Infrared Supercontinuum Spectra Spanning 2–15 μm Using As_2Se_3 Chalcogenide glass Triangular-Core Graded-Index Photonic Crystal Fiber",* Journal of Lightwave Technology, vol. 33, no. 18, pp. 3914–3920, 2015.

[13] J. K. Ranka, R. S. Windeler, and A. J. Stentz, *"Visible continuum generation in air-silica microstructure optical fibers with anomalous dispersion at 800 nm",* Optical Letters, vol. 25, pp. 25-27, 2000.

[14] S Vyas, T Tanabe, M Tiwari, G Singh, *"Broadband Supercontinuum Generation and Raman Response in $Ge_{11.5}As_{24}Se_{64.5}$ based chalcogenide Photonic Crystal Fiber",* IEEE International Conference on Computational Techniques in Information and Communication Technologies, 2016, p. 607-611.

[15] A. Seddon, *"Chalcogenide glasses: A review of their preparation, properties and applications",* Journal of Non-Crystalline Solids, vol. 184, pp. 44-50, 1995.

[16] P. Jamatia, T. S. Saini, A. Kumar, and R. K. Sinha, *"Design and analysis of a highly nonlinear composite photonic crystal fiber for supercontinuum generation: visible to mid-infrared",* Applied Optics, vol. 55, no. 24, p. 6775, 2016.

[17] V.Shiryaev and M.Churbanov, *"Trends and prospects for development of chalcogenide fibers for mid-infrared transmission",* J. Non-Cryst. Solids, vol. 377, pp. 225–230, 2013.

[18] X. Gai, T. H. A. Prasad, S. Madden, D.Y. Choi, R. Wang, D. Bullas, and B. L. Davies, *"Progress in optical waveguides fabricated from chalcogenide glasses",* Opt. Express 18, 26635–26646 (2010).

[19] P. Siwach, A. Kumar, and T. S. Saini, *"Broadband supercontinuum generation spanning 1.5–13 μm in $Ge_{11.5}As_{24}Se_{64.5}$ based chalcogenide glass step index optical fiber",* Optik - International Journal for Light and Electron Optics, vol. 156, pp. 564–570, 2018.

[20] S Vyas, T Tanabe, M Tiwari, G Singh, *"Ultra flat broadband supercontinuum in highly nonlinear $Ge_{11.5}As_{24}Se_{64.5}$ photonic crystal fibers",* Ukrainian Journal of Physical Optics 17 (3), 132-139, August 2015.

[21] Pooja Chauhan, Ajeet Kumar, Yogita Kalra, *"Mid-infrared Broadband supercontinuum generation in a highly nonlinear rectangular core chalcogenide photonic crystal fiber***",** Optical Fiber Technology.2018 Dec 1; 46:174-8.

[22] A.Yang, M. Zhang, L. Li, Y. Wang, B. Zhang, Z. Yang, and D. Tang, *"Ga–Sb–S chalcogenide glasses for mid-infrared applications*", J. Am. Ceram. Soc. 99, pp. 1–4, 2015.

[23] C.R. Petersen, U. Miller, I. Kubat, B. Zhou, S. Dupont, J. Ramsay, T. Benson, S. Sujecki, M. Abdel-Moneim, Z. Tang, D. Furniss, A. Seddon, O. Bang, *"Mid-infrared supercontinuum covering the 1.4-13.3 μm molecular fingerprint region using ultra-high NA chalcogenide step-index fibre",* Nat. Photonics 8 (2014) 830–834.

[24] John A. Jay, "*An overview of micro and macrobending in optical fibers*", WP1212, December 2010.

[25] P. Sakunasinha, S. Suwanarat, S. Chiangga, *"Mid-infrared supercontinuum in a $Ge_{11.5}As_{24}Se_{64.5}$ chalcogenide waveguide",* Proc. of SPIE Vol. 9659, 96591J, DOI: 10.1117/12.2196150, 2015.

[26] P. Ma, D.Y. Choi, Y. Yu, X. Gai, Z. Yang, S. Debbarma, S. Madden, B. Luther-Davies, *"Low-loss chalcogenide waveguides for chemical sensing in the mid-infrared",* Opt. Express 21 (24) (2013) 29927–29937.

[27] J.M. Dudley, J.R Taylor, "*Supercontinuum generation in optical fibers",* Cambridge University Press 2010.

[28] J.M. Dudley, J.R Taylor, "*Ten years of nonlinear optics in photonic crystal fibre - progress and perspectives".*

[29] N.Ravi Teja, M.AneeshBabu, T.R.S.Prasad, T.Ravi, *"Different Types of Dispersions in an Optical Fiber",* International Journal of Scientific and Research Publications, Volume 2, Issue 12, December 2012

[30] Ben Chapman, project report on *"Supercontinuum generation in optical fibres",* September 2010, Photonics Group, Department of Physics, Imperial College London.

[31] https://nptel.ac.in/advanced optical communication/lectures/pdf.

[32] S Vyas, T Tanabe, M Tiwari, G Singh, *"Chalcogenide photonic crystal fiber for ultraflat mid-infrared supercontinuum generation",* Chinese optics letters, 1671-7694/2016/123201(5), Dec 2016.

[33] M. R. Karim, B. M. A. Rahman, and G. P. Agrawal, *"Mid-infrared supercontinuum generation using dispersion-engineered $Ge_{11.5}As_{24}Se_{64.5}$ chalcogenide channel waveguide",* Opt. Express 6903, vol. 23,no. 5 (2015).

[34] J.M. Dudley, S. Coen., *"Numerical simulations and coherence properties of supercontinuum generation in photonic crystal and tapered optical fibers"*, IEEE Journal of Selected Topics in Quantum Electronics, 2002.

[35] Bahaa E. A. Saleh, Malvin Carl Teich., *"Fundamentals of photonics"*, John Wiley& Sons, 1991.

[36] https://www.rfwireless-world.com/types of fibers.html.

[37] Xin Gai, Ting Han, Amrita Prasad, Steve Madden, Duk-Yong Choi, Rongping Wang, Douglas Bulla, Barry Luther-Davies, *"Progress in optical waveguides fabricated from chalcogenide glasses"*, Optics Express, 2010.

[38] Erlei Wang, Jia Li, Jin Li, Quan Cheng, Xiaodong Zhou, Haiming Jiang, *"Flattened and broadband mid-infrared super-continuum generation in As_2Se_3 based holey fiber"*, Optical and Quantum Electronics, 2018.

[39] https://www.rfwireless-world.com/Terminology/What-is-FWM.html.

[40] Katherine J. I. Ember, Marieke A. Hoeve, Sarah L. McAughtrie, Mads S. Bergholt, Benjamin J. Dwyer, Molly M. Stevens, Karen Faulds, Stuart J. Forbes & Colin J. Campbell, *"Raman spectroscopy and regenerative medicine: A Review"*, npj Regenerative Medicine **2**, Article number: 12 (2017).

List of Publications

1. Ankit sharma, Pooja Chauhan, Ajeet Kumar and Than Singh Saini, “Design and analysis of microstructured optical fiber for Supercontinuum generation”, International Conference on Photonics, Metamaterials and Plasmonics (PMP-2019) **(accepted).**

Design and Analysis of Microstructured Optical Fiber for Supercontinuum Generation

Ankit Sharma[1], Pooja Chauhan[1, a)], Ajeet Kumar[1, b)], Yogita Kalra[2] and Than Singh[3]

[1]*Advanced Photonics Simulation Research Laboratory, Department of Applied Physics, Delhi Technological University, Delhi, INDIA*
[2]*TIFAC-Centre of Relevance and Excellence in Fiber Optics and Optical Communication, Department of Applied Physics, Delhi Technological University, Delhi, INDIA*
[3]*Optical Functional Materials Laboratory, Toyota Technological Institute, Nagoya, JAPAN*

[a)] Corresponding author: pooja_ch21@yahoo.com
[b)]ajeetdph@gmail.com

Abstract. A microstructured optical fiber in $Ge_{11.5}As_{24}Se_{64.5}$ chalcogenide glass has been numerically modeled for supercontinuum generation. The proposed design holds all-normal dispersion property and offers very high nonlinear coefficient at a pump wavelength of 2.8 µm.

Introduction

Chalcogenide-basedmicrostructured optical fibers (ch-MOF) are becoming superior in comparison of conventional optical fibers due to their flexibility in engineering dispersion profile, high nonlinear refractive index, and broad optical transparency window in the mid-infrared region [1,2]. Several chalcogenide glasses such as $Ge_{11.5}As_{24}Se_{64.5}$, As_2S_3, As_2Se_3, and $Ge_{11.5}As_{24}S_{64.5}$ are widely in practice for improving the output efficiency of the infrared photonic devices because of their high nonlinearity and need of low threshold power [3].

In our study, we have tailored the geometrical parameter of the proposed ch-MOF in order to achieve an all-normal-dispersion profile and high nonlinearity to get ultra-broadband supercontinuum generation (SCG).

Proposed Ch-MOF Design

The air-holes are arranged symmetrically in a rectangular lattice pattern. We have considered the diameter of air-holes as d in the cladding region made up of $Ge_{11.5}As_{24}Se_{64.5}$ chalcogenide glass and the center to center distance of air-holes is denoted by Λ and taken as constant as 1µm.

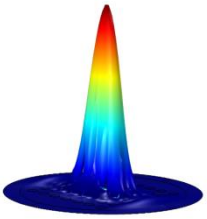

FIGURE 1. Electric field distribution of fundamental mode at a pump wavelength of 2.8 µm.

Results and Discussion

The linear and nonlinear characteristics for the SCG are studied using the finite element method. We have followed the process of optimization of the geometrical parameter i.e., *d* in order to obtain the all-normal dispersion profile.

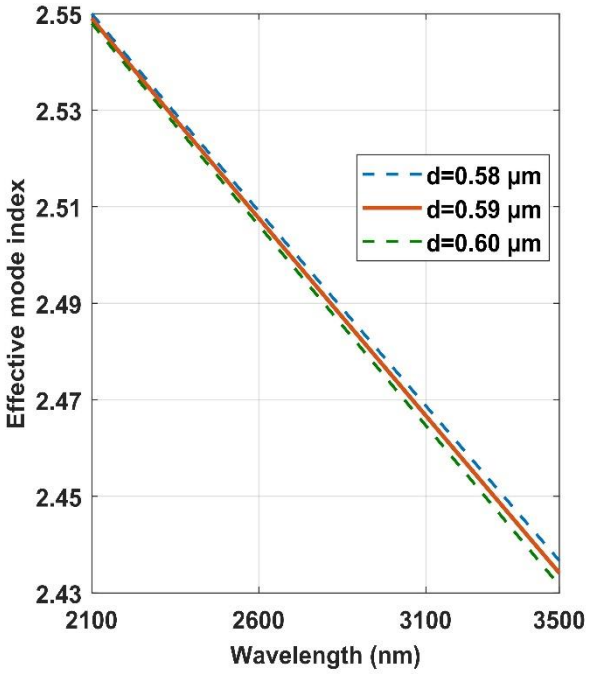

FIGURE 2. Variation of mode index along wavelength.

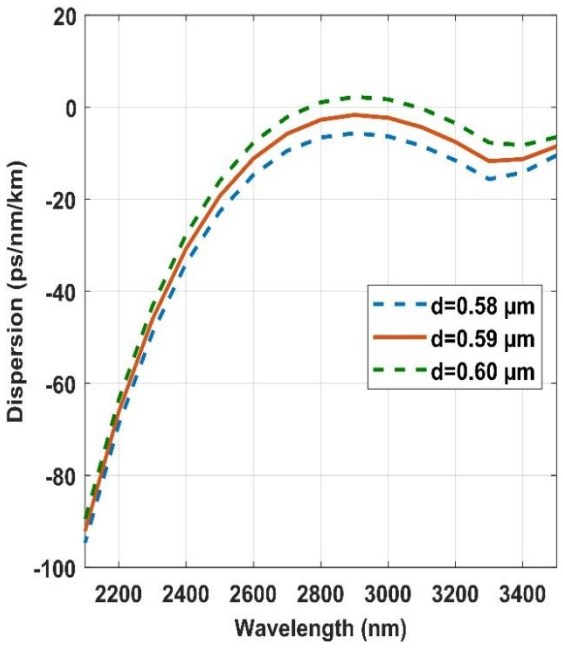

FIGURE 3. Effect of *d* on chromatic dispersion.

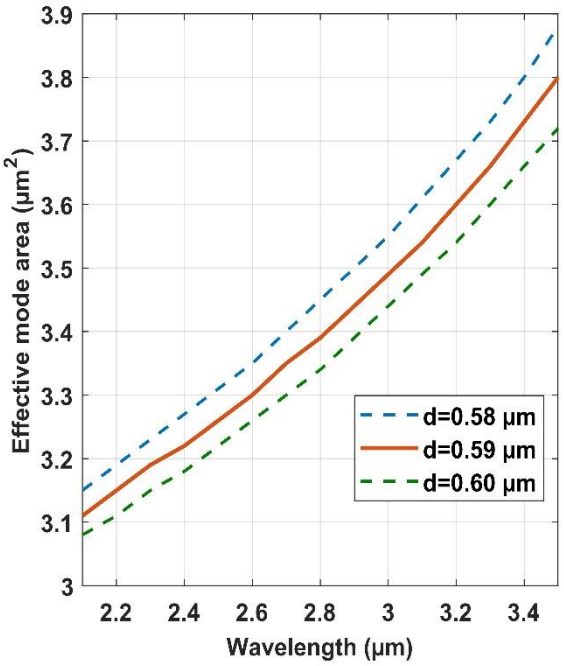

FIGURE 4. Effect of *d* on mode area.

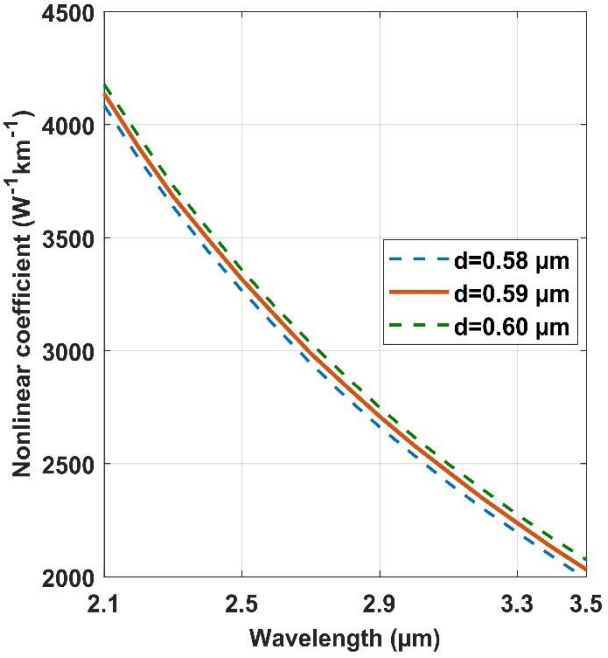

FIGURE 5. Effect of *d* on nonlinearity.

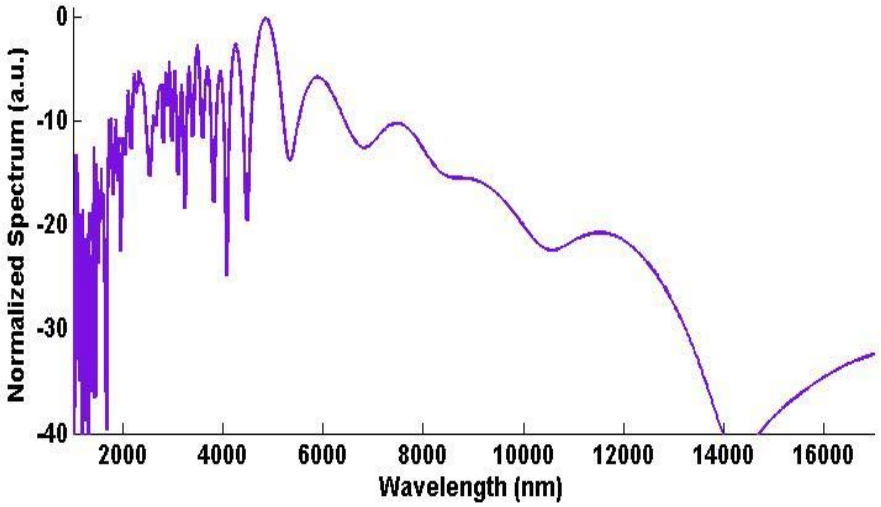

FIGURE 6. SCG spectra

Conclusions

In our study, we have numerically proposed a $Ge_{11.5}As_{24}Se_{64.5}$chalcogenide based microstructured optical fiber for the supercontinuum generation in the mid-infrared region. We have achieved an ultra-broadband supercontinuum spanning, 2-15 µm using a femtosecond laser source in a few millimeters fiber length.

TABLE 1. Optimized parameters with numerically reported results

Optimized dimensions	**Pump Wavelength**	**Dispersion**	**Nonlinear Coefficient**	**Effective Mode Area**	**SCG**
d =0.59 µm;Λ=1 µm	2.8 µm	-2.7 ps/nm/km	2889 $W^{-1}.km^{-1}$	3.39 μm^2	2-14 µm

.

References

1. P. Russell, "Photonic crystal fibers", *Science***299**, 358-362 (2003).
2. J. M. Dudley, G. Genty, and S. Coen, "Supercontinuum generation in photoniccrystal fiber", *Rev. Mod. Phys*. **78**, 1153-1184 (2006).
3. M. R. Karim, B. M. A. Rahman and G. P. Agrawal, "Dispersion engineered Ge-As-Se nanowire for supercontinuum generation: a parametric study", *Opt. Expres***22**. 312029-31040 (2014).